Received: 19 December 2023 | Revised: 17 August 2024 | Accepted: 21 August 2024

DOI: 10.1002/dvdy.735

REVIEW

Developmental Dynamics WILEY

Ventral body wall closure: Mechanistic insights from mouse models and translation to human pathology

Caroline Formstone[1] | **Bashar Aldeiri**[2] | **Mark Davenport**[3] | **Philippa Francis-West**[4]

[1]Department of Clinical, Pharmaceutical and Biological Sciences, University of Hertfordshire, Hatfield, UK

[2]Department of Paediatric Surgery, Chelsea and Westminster Hospital, London, UK

[3]Department of Paediatric Surgery, King's College Hospital, London, UK

[4]Centre for Craniofacial and Regenerative Biology, King's College London, London, UK

Correspondence
Caroline Formstone, Department of Clinical, Pharmaceutical and Biological Sciences, University of Hertfordshire, Hatfield AL10 9AB, UK.
Email: c.formstone@herts.ac.uk

Funding information
Biotechnology and Biological Sciences Research Council, Grant/Award Numbers: BB/G021074/1/BB, BB/W01730X/1; British Heart Foundation, Grant/Award Number: PG/14/1/30549; University of Manchester, Grant/Award Number: 105082; Wellcome Trust, Grant/Award Number: 095824/Z/11/Z

Abstract

The ventral body wall (VBW) that encloses the thoracic and abdominal cavities arises by extensive cell movements and morphogenetic changes during embryonic development. These morphogenetic processes include embryonic folding generating the primary body wall; the initial ventral cover of the embryo, followed by directed mesodermal cell migrations, contributing to the secondary body wall. Clinical anomalies in VBW development affect approximately 1 in 3000 live births. However, the cell interactions and critical cellular behaviors that control VBW development remain little understood. Here, we describe the embryonic origins of the VBW, the cellular and morphogenetic processes, and key genes, that are essential for VBW development. We also provide a clinical overview of VBW anomalies, together with environmental and genetic influences, and discuss the insight gained from over 70 mouse models that exhibit VBW defects, and their relevance, with respect to human pathology. In doing so we propose a phenotypic framework for researchers in the field which takes into account the clinical picture. We also highlight cases where there is a current paucity of mouse models for particular clinical defects and key gaps in knowledge about embryonic VBW development that need to be addressed to further understand mechanisms of human VBW pathologies.

KEYWORDS

bladder or cloacal exstrophy, ectopia cordis, exomphalos, myofibroblasts, thoracoabdominoschisis, ventral body wall development

1 | INTRODUCTION AND AIMS

The ventral body wall (VBW) consists of the skin, dermis, sternum, ribs intercostal and abdominal musculature that enclose the thoracic and abdominal cavities. The VBW arises during embryonic development in two key steps. First, the primary body wall (PBW), consisting of a thin mesodermal/ectodermal layer, covering most of the ventral embryo, except at the level of the umbilicus, is generated during embryonic folding. Second, the PBW is invaded by

Caroline Formstone and Bashar Aldeiri are joint first authors.

the secondary body wall (SBW) comprising of lateral plate and paraxial-mesoderm-derived tissues adjacent to the PBW. "Closure" refers to the process whereby the PBW has been infiltrated by the two opposing SBWs which then meet at the ventral midline of the embryo. The initially large umbilicus or "umbilical ring" (UR) has narrowed to contribute to the umbilical cord. At this point, the VBW is "closed." Anomalies in VBW development include thoracoabdominoschisis (TAS), ectopia cordis, exomphalos, and bladder exstrophy which can accompany pelvic and genital defects (see definition box, Table 1). The most severe of these is TAS, the complete failure to form the VBW, which is incompatible with life. Most VBW defects are sporadic, and the etiology is multifactorial.

This review outlines VBW development and discusses the insight gained from animal models into clinical defects. The review is in four sections: (1) the embryonic origin and morphogenesis of the VBW; (2) the molecular regulation of VBW closure; (3) a clinical description of the different types of body wall closure anomalies, the genetic, and environmental influences where known; and (4) an overview of some mouse models that give insights into the genetic and cellular mechanisms of the various VBW anomalies.

2 | ORIGIN AND MORPHOGENESIS OF THE PRIMARY VBW

2.1 | Definition of the primary VBW

The PBW is an ambiguous term originally introduced to label the VBW in the mouse embryo immediately post-turning.[1] This anatomical description refers to a mesodermal and ectodermal layer that provides ventral cover to the intraembryonic coelom in early organogenesis. Nevertheless, VBW closure is a dynamic process, and different cellular arrangements cover the ventral body organs at different stages during embryogenesis. We will use the term "PBW" to refer to the first mesodermal-ectodermal tissue cover to the intraembryonic coelom in the post-turning embryo.

2.2 | The embryogenesis of the primary VBW

Understanding the embryogenesis of the "primary VBW" in vertebrates requires concurrent understanding of how the discoid shaped embryo folds to take the embryo

TABLE 1 Definition box.

Term	Definition
Abdominal bands	Heterogeneous cell population at leading (most ventral) edge of abdominal SBW
Axes of embryonic development	
Cranial-caudal	Head to tail. Equivalent to anterior–posterior in embryology
Dorso-ventral	"Back to belly." Equivalent to posterior–anterior in clinical definitions
Bladder exstrophy	The bladder is not covered by the VBW
Cloacal exstrophy	The cloaca, the progenitor of the bladder and colon, has not separated and is also not covered by the VBW
Cordis ectopia	The heart is external to the thoracic VBW
Exomphalos	Also known as omphalocele. The midgut (and sometimes the liver) are outside the VBW but contained within the umbilicus
Gastroschisis (GS)	Protrusion of the gastrointestinal tract which is not contained within the umbilicus
Leading edge of VBW	The most ventral edge of the SBW, containing the sternal and abdominal bands
Pentalogy of Cantrell	A group of three to five anomalies that can occur together affecting the heart, diaphragm, and VBW
Planar cell polarity (PCP)	A term used to describe the co-ordinated polarity of cells or co-ordinated collective cell movements within a plane of tissue, that is, convergent-extension and orientated cell divisions.
Primary body wall (PBW)	The first tissue cover, consisting of a thin mesodermal and ectoderm layer, over the ventral surface of the embryo
Secondary body wall (SBW)	The invading paraxial and LPM that will form the definitive VBW
Sternal bands	Heterogeneous cell population at leading (most ventral) edge of thoracic SBW
Thoracoabdominoschisis	An anomaly where the thoracic and abdominal organs are not covered by the VBW
Umbilical ring (UR)	The ectoderm at the junction of the amnion and embryo proper

proper "bean-shaped" configuration. In rodents, but not in human or chick embryos which are flat, this folding is linked to a simultaneous 180-degree embryo rotation around the dorso-ventral axis. Although there is huge variability in the degree to which different vertebrate embryos fold (and turn), the overall process is comparable and results in the creation of body cavities and a PBW (reviewed in Reference 2). The midline is one of the first distinctive regions to form in the developing embryo with the formation of the primitive streak. The dorso-ventral and cranial-caudal axes are defined in the trilaminar discoid-shaped embryo which consists of the three embryonic germ layers, ectoderm, mesoderm, and endoderm (Figure 1A′). Of particular importance for VBW development, the mesoderm starts to form its definitive components, the lateral plate mesoderm (LPM), intermediate mesoderm and paraxial mesoderm (Figure 1A′). Of these mesodermal components, the LPM plays an

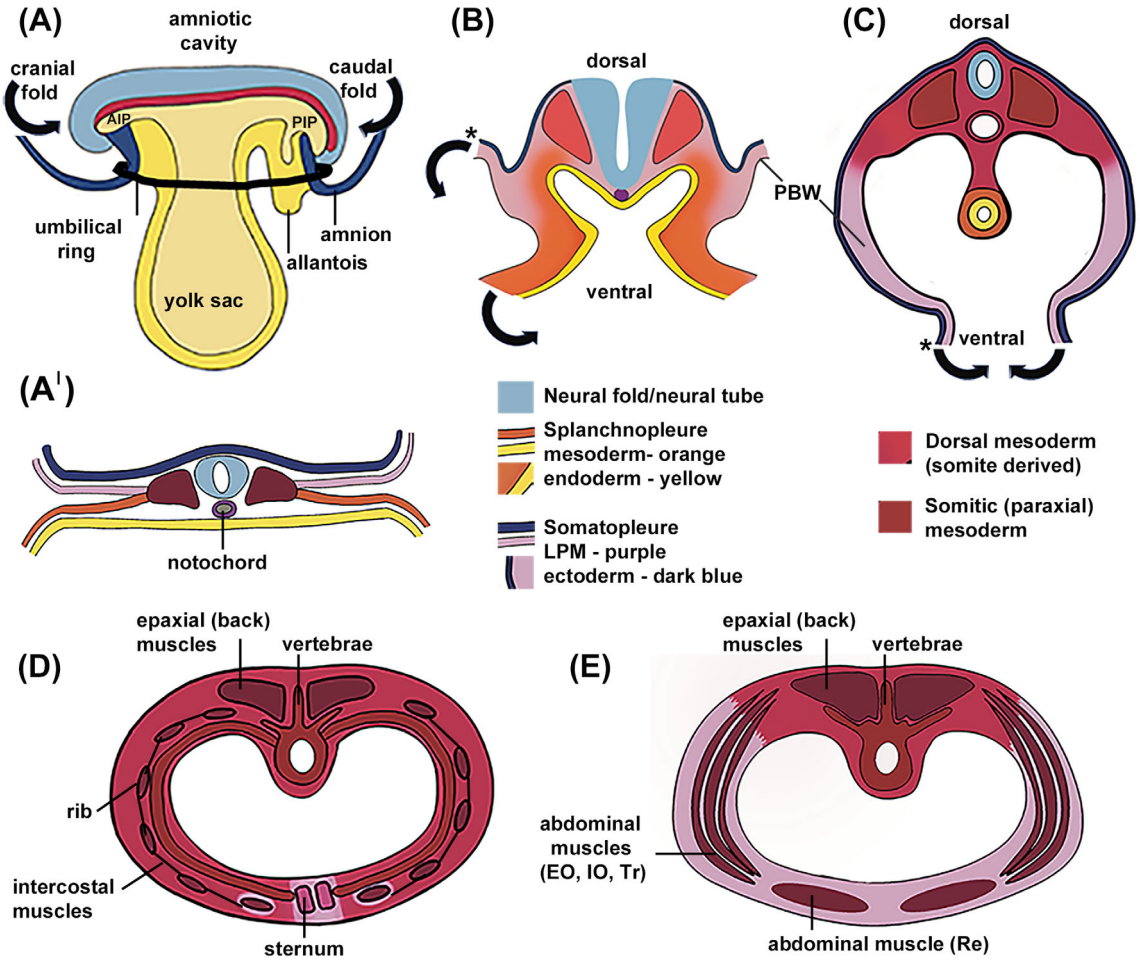

FIGURE 1 Ventral body wall folding and the contribution of the paraxial and lateral plate mesoderm. (A–C) Progression of embryonic folding to generate the primary body wall from the early gastrula stage (A, A′), to later developmental stages, B, and then C. The stages shown are after embryo turning and model VBW closure in humans, mouse and chicks. In embryonic mice, Gata4, Furin, Hand1/2 control, the step shown in (A), Pitx2 the step shown in (B), and Six5/6 the stage shown in (C). (A) A lateral view while (A′, B, C) are transverse sections. The ectoderm is continuous with the amnion and the endoderm is continuous with the yolk sac. The amniotic sac/cavity initially lies above the embryo (A). The embryo folds laterally and along the cranial-caudal axes such that the splanchnopleure is ultimately located in the center of the embryo as a blind ended tube. The somatopleure folds around to enclose the VBW. This somatopleure folding also brings the amnion around the embryo such that the amniotic sac now surrounds the entire embryo. (B, C) * demarcates the position of connection to amnion. (D, E) Schematics of the contribution of the paraxial mesoderm and LPM to the thoracic and abdominal ventral body wall, respectively, based on fate mapping studies in the mouse.[3] The paraxial/LPM contribution varies between species (see Section 3.5) and although not proven, the mouse embryo is anticipated to more closely model human development compared to the chick. The distal intercostal muscles move just ahead of the ribs and become encapsulated by LPM.[3–5] Cranial-caudal and dorso-ventral axes are indicated. Block arrows indicate the direction of folding. AIP, anterior intestinal portal; EO, external oblique muscle, IO, internal oblique muscle, PIP, posterior intestinal portal. Tr, transversus abdominis muscle, Re, rectus abdominis muscle. Schematic (D) shows the human anatomy, panniculus carnosus muscle of mouse embryo is not shown. Outline for (B) and (D, E) based on Beddington and Robertson[6] and Scaal,[7] respectively.

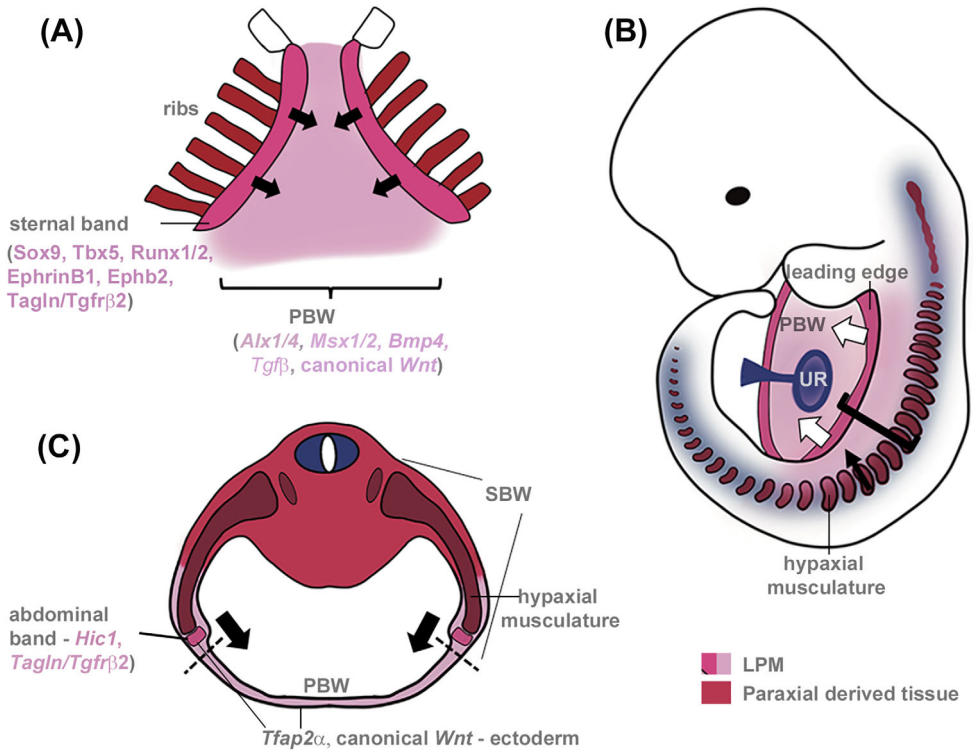

FIGURE 2 Development of the secondary body wall. (A) Frontal, (B) semi-lateral, and (C) transverse views of the mouse developing VBW at stages E12.5 (A, B) and E13.5 (C). The leading edge of the SBW (dark pink) followed by the adjacent tissue invades the PBW. The leading edge contains myofibroblasts that are essential for VBW closure and is ahead of the developing ribs/musculature and innervation which arise from the paraxial mesoderm and neuroectoderm, respectively. In the thoracic SBW, the leading edge also contains the mesosternal precursors. Bracket in (B) indicates SBW. The umbilical ring (UR) is the point of transient physiological herniation of the midgut: Here, a mesodermal layer separates the abdominal cavity of the embryo from the umbilical cord. Block arrows indicate the direction of cell movement. Secreted signals from the PBW control development of both the PBW and SBW. Genes expressed within the leading edge are also essential for advancement of the SBW and VBW closure. Dashed line in (C) indicates boundary between PBW and SBW. PBW, primary body wall, SBW secondary body. Outline for (A) and (C) based on Mao et al.[8] and Nichol et al.,[9] respectively.

essential role in the creation of the first mesodermal cover to ventral embryonic structures (Figures 1A′–E and 2A–C). The LPM divides into a dorsally located somatic leaflet underlying the surface ectoderm (these two layers are referred to as somatopleure) and a ventrally located splanchnic leaf that lines the endoderm (these two layers are referred to as splanchnopleure) (Figure 1A′).

Next, the committed germinal layers organize into definitive organs. In preparation for organogenesis, the embryo is required to provide an enclosed and shielded intraembryonic space to allow for the growth and development of the future organs while separated from the extraembryonic space. The intraembryonic coelom, the space between the splanchnic and somatopleure divisions of the LPM that is allocated for future viscera, is at this stage thin and lies in continuity with the extraembryonic coelom laterally. In addition, the right and left, cranial and caudal portions of this space are not yet in continuity. To accommodate the next stage in development the vertebrate embryo folds along the cranial-caudal and dorso-ventral axes (Figure 1A–C). Folding around the cranial-caudal axis occurs at the anterior (cranial) intestinal portal (AIP) and posterior (caudal) intestinal portal (PIP), respectively (Figure 1A). In rodents and chicks, it is thought that the higher proliferation in the left somatopleure and splanchnopleure (compared to the right side) together with the attachment to the extraembryonic membrane is essential for dorso-ventral folding.[10–12]

At the end of the folding process, the endoderm sits within the cavity of the intraembryonic coelom, covered by the splanchnic mesoderm (Figure 1C), and the various elements of the intraembryonic coelom are now adjacent to one another. The amniotic membrane, which is continuous with the somatopleure, now surrounds the embryo on both its dorsal and ventral surfaces. The four folds of the somatopleure form the PBW, the first cover of the intraembryonic coelom, separating it from the amniotic cavity (Figure 1B,C). The only connection between the intraembryonic coelom and the extraembryonic coelom is at the edges of the yolk sac, and this will in turn completely separate when full ventral midline closure ensues. The folding somatopleure edges of the embryo where they connect with the amniotic

membranes is called the UR (Figures 1A and 2B). The umbilical ring (UR) is the site of a thickened domain of ectoderm, which undergoes ectodermal apoptosis, epithelial-mesenchymal transformation (EMT), and cell deposition.

3 | ORIGIN AND MORPHOGENESIS OF THE SECONDARY VBW

3.1 | Definitions and origin of the secondary VBW

The SBW constitutes the skin, ribs, sternum as well as the thoracic, abdominal and pelvic musculature and connective tissues. During development, the SBW is defined as the tissues, including the musculoskeletal components, that will invade the PBW. The SBW has three embryonic origins: the paraxial (somitic) mesoderm and LPM (somatopleure, also called somatic layer) together with the overlying ectoderm. The paraxial mesoderm forms the ribs, hypaxial musculature (the abdominal and intercostal muscles), and contributes to the dermis of the skin (Figure 1D,E).[13–18] The LPM gives rise to the sternum, and also contributes to the dermis of the VBW (Figure 1D)[3,19,20]; reviewed by.[7] The relative contributions of the LPM and paraxial mesoderm to the VBW dermis, and connective tissues varies along the cranial–caudal axis (see Figure 1D,E and Section 3.5). The LPM also gives rise to the pelvic girdle (ilium, ischium, pubis).[21] Although the pelvic girdle is not a VBW derivative, it can be affected by VBW anomalies.

3.2 | Formation and morphogenesis of the VBW skeleton

The ribs develop from the sclerotome portion of the somite (paraxial mesoderm) and can be divided into two domains, the proximal (costal head, neck, and tubercles) and distal rib shaft which arise from different regions of the sclerotome (reviewed by Scaal[7]). Different developmental networks control proximal versus distal rib formation. This is clearly shown by mouse mutants; the *Pax1* mutant, *undulated*, lacks the proximal ribs whereas in *Pax3*, *Splotch*, mutants, the distal ribs fail to form.[22–24] Distal rib extension and differentiation requires signals from the PBW ectoderm and the adjacent developing intercostal musculature (Figure 2A).[18,25]

The sternum develops independently of the ribs and requires signals from the overlying ectoderm.[18,19] Anatomically and developmentally the sternum is divided into three domains: the presternum (or manubrium), the mesosternum (or body of sternum), and the xiphoid process. In humans and mice the presternum arises from multiple cartilage condensations and may also receive contributions from the neural crest while the mesosternum arises from the "sternal bands" contained within the leading most ventral edge of the SBW (see Figure 2A and Section 4.2.2).[19,20,26–28] In the E12.5–E13.5 mouse embryo, the sternal bands can be visualized as a condensation of densely-packed cells which express chondrogenic and osteogenic markers.[4,8] In mice, the two opposing sternal bars meet at the midline by E14.5 after which they undergo cartilage differentiation.

3.3 | Formation and morphogenesis of the VBW musculature

Studies in chick and mouse indicate VBW musculature arises from the hypaxial myotome in the somite and that the myotome extends into the VBW (Figures 1D,E and 2B,C).[29,30] This muscle mass becomes histologically visible around day 33 (CS15) of human development.[31,32] By day 48 (CS19) muscle progenitors have covered 50% of the distance toward the ventral midline and by day 54 (CS 21) have reached the ventral midline to surround the UR. The abdominus rectus muscle and rectus sheath clearly abut the UR by day 56 (CS23).[31,32]

Studies in mouse embryos reveal a similar overall pattern of development but muscle development occurs earlier in the human embryo when compared to the mouse embryo. Myotomal extension starts at E11.5 and by E14.5 myoblasts have reached the ventral midline. Mice develop an additional abdominal muscle layer, the panniculus carnosus (PC), which lags slightly behind the other abdominal muscles, both temporally and spatially[9] and ultimately sits directly under the skin to enable skin "twitching" (reviewed by Naldaiz-Gastesi et al.[33]).

3.4 | Formation and morphogenesis of the skin

In the mouse trunk, the primary establishment of the epidermis initiates around E13.5 at the mid-flank.[34–36] Just prior to this, the mid-flank surface ectoderm thickens and consists of flattened squamous-like cells, which form a ridge.[34,35,37] The disorganized, thickened, mid-flank ectoderm then undergoes an "outside-in" (radial) intercalation generating an organized epidermis, consisting of cuboidal cells, which spread dorsally and ventrally fully enclosing the abdomen by E16.[36] Explant experiments demonstrated that this radial intercalation is tissue intrinsic.[36] While the signals responsible for epidermis induction are unknown,

the site of the future mid-flank ectodermal thickening at E13.25 is labeled at E12.5 by *Tbx15* expression in the loose mesenchyme underlying the dermis and the most ventral position of the extending myotome. Notably, *Tbx15* expression also expands both dorsally and ventrally in a pattern resembling the formation of the epidermis.[38] Munger and Munger have proposed that initiation of ectodermal differentiation coincides with the migration of sternal and abdominal bands, that is, the leading ventral edge of the SBW and subcutaneous innervation[35] (also see Section 4.2.2). In the mouse VBW, dermal differentiation begins at E11.5 at the same time as myotomal extension and the first switch in ectodermal keratin expression, and is dependent upon Wnt/β-catenin signaling.[39–41]

3.5 | Differential contribution of the paraxial and LPM to the thoracic and abdominal VBW

The VBW consists of both paraxial mesoderm and LPM-derived tissues. To define the spatial relationship between these two mesodermal populations and to determine the differential contribution to growth, Nowicki and colleagues (2003) performed fate mapping of somitic (paraxial) mesoderm precursors within the thoracic body wall using orthotopic chick-quail chimaeras.[15] The epaxial (back) muscle progenitors and proximal hypaxial (intercostal) musculature, together with proximal rib precursors, were visualized as a collective dense population of labeled quail somitic precursors showing that they, together with their connective tissues, are paraxial-mesoderm-derived tissues. This is in contrast to the dilution of the ventral most labeled quail somitic precursors marking the distal developing hypaxial (intercostal) muscles and sternal ribs as they intermingled with unlabeled LPM of chick origin. As labeled quail somitic cells encroach into the LPM, the muscle precursors begin to differentiate within the LPM environment.

In the mouse, the relative contribution of the paraxial mesoderm versus LPM has been determined using a *Prx1* reporter mouse which labels cells of the LPM lineage.[3] This shows that the paraxial mesoderm and LPM contributions are slightly different to that of the chick. In the mouse thorax, only the distal part of the first rib and the distal intercostal muscles are surrounded by LPM-derived connective tissues (Figure 1D). This study also showed different relative contributions of the LPM to the thoracic versus the abdominal VBW. In the mouse abdomen, the hypaxial musculature is surrounded by LPM except in the most proximal (dorsal) region[3] (Figure 1E). Thus, the LPM expands significantly in the abdomen compared to its more limited contribution to the thoracic VBW. As the LPM can influence gene expression of the invading paraxial mesoderm cells,[42] the LPM would be predicted to play a more significant role in the patterning and morphogenesis of the abdominal musculature compared to the musculature of the thorax. For example, gene mutations that affect LPM would not only influence LPM-derived tissues, such as the sternum, but can impact the development of adjacent paraxial-mesoderm-derived tissues such as the distal ribs (reviewed by Burke et al.[43]).

3.6 | Closure of the VBW

Closure is defined as when the two opposing ventral SBWs have migrated into the PBW to meet at the midline and the UR has narrowed to contribute to the definitive umbilical cord (Figures 1D,E and 2A–C). Abdominal VBW closure, occurs after the midgut has undergone a transient physiological herniation into the umbilicus (between E13.5 and E15.5 in mice and weeks 5–10 in humans). The first point of contact of the opposing ventral SBW leading edges is in the most cranial region of the thoracic wall at the level of the clavicles (E12.5 in mice). Fate mapping studies of the closing secondary thoracic body wall in in vitro explant culture have shown that the ectoderm and mesenchyme move together.[26] VBW closure proceeds in a caudal direction and, in mice, the thoracic wall is completely closed by E14.5. Closure then also proceeds cranially from the infra-umbilical region such that closure is now bidirectional. The final point of closure of the VBW is at the level of the umbilicus, that is, the UR occurring at E16.5 in mice and week 10 in humans (Figure 2B). Filamentous actin present in the cells of the UR may be essential for this final closure: in *Rock1*$^{-/-}$ mutants in which the VBW does not close, the thickened ridge of ectoderm characteristic of the UR is absent and there is decreased actin staining.[9,44,45]

The VBW can close in vivo in the absence of the ribs or a differentiated body wall musculature.[46–48] For example, hypoplasia of the ribs, such as in Campomelic dysplasia does not prevent thoracic body wall closure[23,49] (OMIM 114290). This indicates that the ribs and body wall musculature per se are not necessary, suggesting that another cell population may be required. One candidate is the myofibroblasts, as discussed in Section 4.2.3.

It is also important to note that while many processes may be identical during closure of the thoracic and abdominal wall (such as the requirement for Tgfβ and Wnt signaling), the relative contribution of the paraxial mesoderm and LPM differs (see Section 3.5 and Figure 1D,E), collective cell movements vary and there

TABLE 2 Summary of genes/pathways implicated in VBW development.

Disrupted gene/ pathway	VBW phenotype	Gene/pathway information and mechanisms
Transcription/DNA binding factors		
Alx4	Exomphalos, pubic diastasis, BE-like	Paired type homeodomain, expressed in PBW at E9.5-E12.5, decreasing later. 100% penetrance exomphalos.[50–52] Mechanism: increase in HH signaling in abdominal VBW and decreased mesenchymal migration caudally into the pelvic region.[50] Also see Increased Shh signaling in Table and discussion in Sections 3.7 and 6.5.
Alx1*(*Cart1*)*/Alx4	Exomphalos, Split sternum	Alx1 and Alx4 functionally overlap, both are expressed in PBW mesenchyme.[52,53] *Alx1* nulls do not have an exomphalos or a split sternum phenotype.[54,55] Exomphalos phenotype of *Alx4* null is not modified by additional *Alx1* null alleles but thoracic wall closure affected indicated by a split sternum. No evidence of disrupted hedgehog signaling in VBW.[53]
***AP2α* (*Tfap2α*)**	TAS	Expressed in PBW and SBW ectoderm. PBW ruptures by E13.5 resulting in lack of cover for ventral body, SBW formation fails.[56–59] See Sections 4, 4.2.2, and 6.1.
***Ataxin1/Ataxin-1-like* (*Atxn1/1 L*)**	Exomphalos	Binds DNA/RNA. May interact with Capicua (cic) in nucleus, see below.[60]
Barx1	GS	Model: overexpression of Barx1 in mesenchyme/gut sub-mucosa leads to 100% penetrance of persistent intestinal herniation. Potential mechanism: failure of appropriate mid-gut morphogenesis and rotation.[61]
***Capicua* (*cic*)**	Exomphalos	HMG-box containing transcriptional repressor. May interact with **Atxn1/1 L** in nucleus, see above.[62]
Gli3	Split sternum, Exomphalos, pubic diastasis	Hedgehog signaling transcriptional component, inhibits Shh signaling.[63,64] Mechanism: ectopic/increased HH signaling in VBW from E9.5 to E12.5 and increased apoptosis.[63] Also see "Increased Shh signaling" in Table and Section 6.5.
***AHDC1* (Gibbin protein)**	Exomphalos	AT-hook DNA binding protein involved in mesoderm and ectoderm patterning.[65]
Glucocorticoid receptor	Exomphalos	Nuclear hormone receptor, essential for metabolism and growth. Model: mesenchymal loss of Glucocorticoid receptor expression leads to 100% penetrance of phenotype. Potential mechanism: mechanical defect as elastin and collagen levels and organization are disrupted in umbilical area.[66]
***Grainyhead-like 2* (*Grhl2*)**	Open thoracic and abdominal body wall	Expressed in non-neural ectoderm. Potential mechanism: modulation of epithelial cell shape, junctions and tissue mechanics.[67,68] Also see Section 6.1.
Hand1	GS	Basic helix–loop–helix (bHLH) type transcription factor, expressed in extra-embryonic mesoderm and entire PBW but later restricts to umbilical ring. Model: conditional deletion in LPM. Proposed mechanism: disrupted development of LPM derivatives.[69] See Sections 4.1 and 6.3
Hic1*, *hypermethylated in cancer	Exomphalos	Pox virus zinc-finger (POZ) domain containing protein. Expressed in somites at E10.5 and at leading edge of SBW by E11.5.[70,71] Fate mapping studies reveal limb *Hic1* expressing cells are of somitic origin suggesting same origin for *Hic1*-expressing mesenchyme within VBW.[72] Function unknown. Also see[73] and Sections 4.2.2 and 4.2.3.

(Continues)

TABLE 2 (Continued)

Disrupted gene/ pathway	VBW phenotype	Gene/pathway information and mechanisms
Hoxb2/Hoxb4	Split sternum, PC	Homeobox. Proposed mechanism: disruption to PBW by E11 with decreased *Alx3/4* expression, a thinner PBW by E11.5 and a failure of SBW invasion.[74–76] Also see Section 6.1 and References 74 and 76
Msx1/Msx2	LBWC, Exomphalos	Homeobox type, PBW mesenchymal expression and SBW musculature. Proposed mechanism: defective PBW signaling and stalling of SBW enclosure.[77] Also see Section 6.1.
p63	BE	Ectoderm master regulator expressed in ectoderm, urogenital sinus and tail bud at E11.5.[78] Strong expression of a dominant negative ΔNp63 isoform in ventral bladder epithelium where it exerts an anti-apoptotic effect and controls development of adjacent splanchnic mesoderm.[78] See Section 6.5 for further discussion.
Pitx2	LBWC	Homeobox type, participates in left–right asymmetry and tissue pattern formation. Asymmetric expression on left side of somatopleure LPM, also expressed in SBW myotome.[79] Mechanism: failure of somatopleure folding and PBW formation with altered expression of *Hox* and *Tbx* family members.[80–85] See discussions 4.1, 6.1, and 6.2.
Runx1/Runx2	Open thoracic wall/EC	*Runx1* and *-2* highly expressed at E12.5 and E13.5 in sternal band of SBW.[4] Proposed mechanism: failure of thoracic SBW to invade thoracic PBW. PBW ruptures. Also see Section 4.2.2.
Six4/Six5	Exomphalos	Homeobox type, expressed in PBW ectoderm, LPM and mesothelial precursor cells. **100%** penetrance exomphalos exhibited by double homozygote null. Mechanism: defective somatopleure/PBW morphogenesis with decreased proliferation in ectoderm (both sides) and mesoderm (right hand side only) at E10.5 as well as decreased cell survival overall.[86] Also see Section 4.1.
Sox C* subfamily *Sox4*, *Sox11*, *and Sox12	Split sternum, Exomphalos	HMG-type. *Sox11* is expressed early in somitic mesoderm (E10.5–E11.5).[87] *Sox11* mutants have exomphalos.[88] There is redundancy with Sox4 and Sox12: $Sox11^{+/-}/Sox4^{+/-}$ embryos have exomphalos while additional loss of *Sox12*, also results in a split sternum.[89] Proposed mechanism within VBW: decreased cell survival and proliferation or loss of somitic contribution to VBW.
Zic3	LBWC (low penetrance)	Zinc finger type transcription factor deleted in *Bent tail* mouse mutant. Zic3 determines L-R asymmetry.[90] Potential turning defect, very low penetrance of VBW defect at E15.5.[91] Note *Zic3* nulls do not have a VBW defect[90] indicating Zic3 may be a modifier gene increasing the risk of a VBW defect when together with other gene mutations and /or environmental factors.
Extracellular signaling ligands and receptors		
BMP signaling *Alk3* (receptor) *Bmp2* and *Bmp4* (ligands)	Split sternum, Open thoracic wall Exomphalos	Cardinal signaling pathway for embryonic growth and differentiation. Redundancy between Bmp2 and Bmp4 with dosage-dependent phenotypes ranging from a Split Xiphoid (*Bmp2* or Bmp4 heterozygotes) to exomphalos (*Bmp2/Bmp4* double heterozygotes; hypomorphic *Bmp2* mutant) to an open thoracic and abdominal wall (*Bmp4* deficient embryos).[92–94] Potential mechanism: PBW forms normally but *Alk3* mesoderm specific null suggests BMP signaling role from PBW to drive SBW development.[95] Reduction in Bmp signaling in VBW and in gastrointestinal tract affecting gut looping in chick also results in VBW defects.[96] Bmp2/4 may also regulate *Msx1/Msx2* expression in PBW. Also see Section 6.6.

TABLE 2 (Continued)

Disrupted gene/ pathway	VBW phenotype	Gene/pathway information and mechanisms
TGFβ signaling *Tgfβr2, Alk5* (receptors) *Tgfβ2/Tgfβ3* (ligands)	Open thoracic and abdominal wall: Failure of entire SBW development	Cardinal signaling pathway for embryonic growth and differentiation. Failure of thoracic and abdominal wall SBW development. 100% penetrance in *Tgfβ2/Tgfβ3* double null embryos,[97] *Alk5* (*Tgfβr1*) -mesenchyme specific deletion[98] and *Tgfβr2* conditional null in ventral myofibroblasts.[99,100] *Tgfβ2* null—split sternum.[101] Potential mechanism: Tgfβ signaling from PBW is essential for function of a population of SBW leading edge myofibroblasts.[99,100] See Sections 4.2.2, 4.2.3, and 6.1 for further discussion.
EphrinB and EphB signaling *Ephrin B1 and EphB2/EphB3*	Delayed fusion of sternum Exomphalos	Membrane anchored signaling at cell–cell contacts. Role in cell adhesion/cell sorting/migration via regulation of cytoskeletal dynamics. In VBW EphB transmembrane proteins act as ligands to activate reverse signaling by Ephrin B transmembrane proteins.[102,103] *EphB2, EphB3 and EphrinB1* expression observed at the leading edge of SBW.[102,104] Knockout studies; phenotype in *EphrinB1*$^{+/-}$ females but not males.[104] *EphB2/EphB3* double mutants.[17,102] Cre inactivation studies indicate likely origin of essential EphrinB1 cells is somitic mesoderm.[103,104] See Sections 4.2.2 and 4.2.3 for critical roles of somitic-derived cells at VBW leading edge.
FGF signaling *Fgf8/9/17/18* (ligands) *Fgfr1 and Fgfr2* (*receptors*)	Exomphalos	Cardinal cell signaling pathway for embryonic growth and tissue differentiation. *Fgfr1* and *Fgfr2* expression: somites, abdominal PBW and SBW.[105] Proposed mechanism for *Fgfr1*/*Fgfr2*: Defective signal from PBW resulting in thickening of dermis and underlying connective tissues within SBW as a consequence of stalled ventral-ward movement of SBW.[105] Phenotype resembles *Hoxb4* mutants. See also MAPK signaling Fgf8,17,18 ligand inactivation show key functions in presomitic and somitic mesoderm necessary for VBW closure. It is proposed that the smaller somites contribute fewer cells (muscle, migratory cells) to the SBW.[106]
Furin	Open ventral body	Serine protease involved in processing of secreted proteins and membrane proteins including **Tgfβ/Bmp** family members. Expressed in AIP and PIP at E8.5. Mechanism: Failure of somatopleure folding to form PBW.[107] Does not recapitulate recognized human pathology. See Section 4.1.
***IGFII* over-expression**	Split sternum, Exomphalos	Ligand required for embryonic growth. 91% penetrance of exomphalos. Also see Section 6.1. Proposed mechanism: organ over-growth e.g. enlarged liver and heart (organomegaly) disrupts body wall morphogenesis. However, also disrupted eyelid and palate fusion suggesting possible underlying defect in tissue movement/tissue fusion processes.[108]
***Pdgf* Pdgfrα (receptor)**	Short split sternum, Exomphalos	Tyrosine kinase receptor. PDGFRα expressed in PBW and somitic derivatives.[109–111] Proposed mechanism: stalled SBW differentiation and ventral-ward movement[111–113] linked to increased cell death in somitic mesoderm and E9.5–E11.5 VBW.[112,114] Activates PI3K intracellular pathway to control VBW development.[115]
Increased SHH signaling	Exomphalos, pubic diastasis	Cardinal cell signaling pathway for embryonic growth and tissue differentiation. Proposed mechanism: graded increase in SHH signaling as reported for compound allelic series of *Gli3* coupled to ***Alx4*** mutant alleles—observe increased penetrance of phenotype.[63] Recovery of phenotype achieved through additional removal of one allele of *Shh*. Ectopic

(Continues)

TABLE 2 (Continued)

Disrupted gene/ pathway	VBW phenotype	Gene/pathway information and mechanisms
		induction of SHH signaling also reported in R*26-SmoM2*:*CAGG cre-ER* mice (constitutively active Smoothened) which led to disorganized hypoplastic abdominal muscles and excessive cell death in VBW at E12.5 associated with an enlarged umbilical ring.[63] Also see SuFu and Section 6.5.
Wnt Signaling **Wls** **Lrp5/6 receptors** **Porcupine**	Ectopia cordis, Split sternum, Exomphalos, Bladder exstrophy-like	Cardinal cell signaling pathway for embryonic growth and tissue differentiation. Mouse models; Wls, essential for Wnt ligand secretion; Lrp5/Lrp6, core obligatory membrane proteins for canonical Wnt signaling; Porcupine (Porcn), acyltransferase enzyme, essential for Wnt ligand palmitoylation and function. A variety of Wnts (canonical and non-canonical) are expressed within the mesenchyme and ectoderm of PBW and SBW.[49,116] Canonical Wnt signaling is active in the PBW and SBW midline.[39,49] Ectodermal and mesenchymal Wnt ligands control PBW morphogenesis and SBW mesenchymal cell survival, proliferation, migration and dermal/myogenic differentiation.[49,116–118] Also see Sections 4.2.4, 6.1, and 6.2 together with Wnt5a and β-catenin in Table.
Tissue polarity and non-canonical Wnt		
Fat4, Dchs1	Wider, thinner and shorter sternum	Protocadherins Fat4 and Dchs1 are a receptor-ligand pair expressed in sternal bands. Mechanism: control of collective cell intercalation behaviors.[8] See Section 3.7.
Celsr1	Exomphalos	Adhesion-GPCR, seven-pass transmembrane protein with key role in core Frizzled-PCP. Expressed in ectoderm and epidermis throughout development.[119] Disruption to epidermal morphogenesis.[36] Genetic interaction with ***Vangl2*** (*loop-tail*) and ***Scribble.***[120] See Sections 4.2.4 and 6.1.
Scribble	LBWC, Exomphalos	Apico-basal polarity determinant associated with Frizzled-PCP signaling in mammals. Expressed in somitic mesoderm, PBW mesenchyme, ectoderm/epidermis of VBW at E13.5.[121] Range of phenotypes from exomphalos to shortened and skewed body axis with open abdominal VBW.[120–124] Genetic interaction with ***Vangl2*** (*loop-tail*) and ***Celsr1.***[120,123] See Sections 4.2.4 and 6.1.
Ptk7	LBWC	Unusual receptor protein tyrosine kinase associated with Frizzled-PCP signaling in mammals but also regulates canonical Wnt signaling. Shortened and skewed body axis and truncated hindlimbs associated with open abdominal VBW.[125,126] See Sections 4.2.4 and 6.1.
Vangl2	LBWC	Key component of Frizzled-PCP, four-pass transmembrane protein. Shortened and skewed body axis and truncated limbs associated with open abdominal VBW. Genetic interaction with ***Ryk,***[127] ***Celsrl*** and ***Scribble.***[120,123] See Sections 4.2.4 and 6.1.
Ryk	LBWC	Receptor tyrosine kinase type but catalytically inactive Wnt receptor, part of Wnt-PCP pathway. *Ryk* null-no phenotype but loss of *Ryk* enhances severity of *Vangl2* heterozygous or *Vangl2* null phenotype, that is, the shortening of body axis, limb truncation and exomphalos.[127] See Sections 4.2.4 and 6.1.
Ror1/Ror2	Delayed SBW closure	Receptor tyrosine kinases and Wnt receptors, part of Wnt-PCP pathway. Truncated cranial-caudal axis and limb anomalies in *Ror1/Ror2* double mutants, resembling *Wnt5a* null mutants.[128,129] Evidence of delayed VBW closure. Mechanism unknown but **Wnt5a-Ror** signaling drives coordinated tissue movements. See Sections 4.2.4 and 6.1.

TABLE 2 (Continued)

Disrupted gene/ pathway	VBW phenotype	Gene/pathway information and mechanisms
Wnt5a	Delay in SBW formation Split sternum	Proposed non-canonical Wnt. Expressed at leading edge of SBW at E11.5–E12.5.[116,130] Truncated cranial-caudal axis, shortened limbs, split sternum.[127,130] Evidence of altered migration and delayed SBW morphogenesis.[49,128] See Sections 4.2.4 and 6.1.
Other membrane proteins		
Podocalyxin (PODXL) mPCLP-1	Exomphalos, delayed closure of PUH	Heavily sialylated/sulfated membrane protein, downstream target of **Pitx2.**[82] 93% penetrance exomphalos up to E17 reducing to 30% for newborn pups. *Podxl*$^{+/-}$ embryos also show delayed closure of physiological hernia but this is resolved before birth. Proposed mechanism: authors speculate Podxl function in mesothelial cells of the peritoneal lining is antiadhesive facilitating midgut retraction into abdominal cavity.[131]
Tmem67 (Meckelin)	Exomphalos	Frizzled-like protein, integral part of the primary cilium. Proposed mechanism: plays a role in **Wnt5a/Ror2** signaling.[132]
Extracellular matrix remodeling		
***Aortic carboxypeptidase-like protein* (*ACLP*)**	GS	Secreted protein that interacts with ECM, expressed in dermis, increases tensile strength of collagen fibers. 100% penetrance of abdominal wall defect reported by References 133,134. Potential mechanism: mechanical defect of dermis. Defect at midline—does not model asymmetric GS phenotype in humans. See Section 6.3.
Bmp1 (mammalian Tolloid-like)	GS	Metalloproteinase. Expressed in LPM of somatopleure at E11.5. Potential mechanism: disruption to **TGFβ** signaling and ECM/collagen formation in dermis/connective tissues of PBW. Amnion "loop" that folds around herniated midgut is not present-therefore defect arises early, is not asymmetrical and does not model GS in humans.[135] See Section 6.3.
Intracellular proteins		
***β-catenin* (*core canonical Wnt component*)**	Delayed closure of PUH	***β-catenin*:** Signaling hub for canonical Wnt signaling as well as cadherin-based cell adhesion. Canonical Wnt signaling is active in PBW and SBW.[39,49] Mechanism: required for proliferation, differentiation, and survival of VBW mesenchyme.[39,40] Zhu et al.[136] also suggest that *β-catenin* regulates contribution of LPM to limbs versus abdomen which impacts rate of SBW closure.
Calreticulin	Exomphalos	ER Ca2+ binding multifunctional protein.[137] Also can impact on growth factor signaling such as Wnt and Bmps.[138,139] Increased expression of pro-apoptotic proteins p53 and Bax within umbilical membrane at E14.5.[140] Proposed mechanism: Increased cell death and altered cell migration
***Dermatan Sulphate Epimerase 1* (*Dse1*)**	Exomphalos	Enzyme that converts Glucaronic Acid to Iduronic Acid (IdoA) in Dermatan Sulphate (DS). DS is mainly found in the extracellular matrix as a component of proteoglycans. IdoA containing ECM induces cell migration and proliferation.[141,142] Proposed mechanism: disruption to dermal collagen maturation[143,144] and/or epidermal morphogenesis.[143]
***Filamin A* (*Flna*)**	Split sternum, Exomphalos	Actin binding and scaffolding protein, X-linked and widely expressed. Phenotype present in male *Flna* hemizygous mutant; sternal defect also seen in *Flna* mutant females.[145,146] Underdevelopment of dermis and muscle, decreased proliferation of VBW leading to a thinner VBW.[145]

(Continues)

TABLE 2 (Continued)

Disrupted gene/ pathway	VBW phenotype	Gene/pathway information and mechanisms
Filamin A/Formin2 (fmn2)	Complete failure of SBW development	Formin-2 is an actin nucleating protein which can function with Flna. *Filamin* null phenotype more severe in simultaneous absence of *Fmn2* resulting in Thoracoabdominoschisis phenotype.[145] Decreased proliferation and malformations in skeleton and musculature. Proposed mechanism: Defect in midline tissue fusion and defective growth and differentiation of the SBW. See Section 6.6.
Folate binding protein-1	GS	Folate receptor. Proposed mechanism: Defect in folate metabolism. High dietary folate supplementation in mutant reduces penetrance of VBW defect.[147] See Section 6.3.
Hrs	Open ventral body	Vesicular transport protein, ubiquitously expressed. Mechanism: failure of somatopleure folding. Embryo remains outside yolk sac. Increased cell death primarily in definitive endoderm at E8.5, the time of embryonic folding. Embryonic lethal by E11.[148]
***Trip11* (GMAP-210)**	Exomphalos	Golgi microtubule associated protein −210. Unknown role in VBW.[149,150]
Male-abnormal 21 like2 Mab21l2	Complete failure of SBW development	Cell fate determinant. *Mab21l2* is expressed in PBW at E9.5–E11.5.[151] Interacts with **Tgfβ/Bmp** signaling.[152] Reduced cell number in PBW from E10.5, thinner PBW linked to decreased proliferation at E11.5. Embryonic lethal by E14.5.[151]
Marcks	Exomphalos	Calmodulin and actin binding protein.[153]
Mek1/Mek2	Exomphalos	MAPK signaling pathway. Model: *Mek1* (*Map2k1*) mesenchymal inactivation in a *Mek2* (*Map2k2*) null background;100% penetrance, PBW forms but SBW does not develop appropriately.[154]
Mekk4	GS	MAPK signaling pathway. Mekk4 (Mapk3) signals to p38 and JNK to regulate cell signaling and actin dynamics. Kinase inactive Mekk4 with dominant-negative activity results in GS.[155] GS not observed in *Mekk4* null embryos.[156]
***p57kip2* (*CDKN1C*)**	Split Sternum Exomphalos, Umbilical hernia	Negative regulator of cell cycle. Delayed thoracic SBW closure, abdominal muscle migration, and skin differentiation.[157] See Section 6.1.
Presenilin-1	Umbilical hernia	Multi-pass ER/Golgi transmembrane protein. *Presenilin-1* mouse mutants reported to exhibit intestinal herniation.[158]
SuFu	Split Sternum, Exomphalos	Negative regulator of **HH** signaling. Hypomorphic allele, 96% penetrant Exomphalos at E18.5. Proposed mechanism: Disruption in HH signaling.[159]
Cytoskeletal components		
Caldesmon Smooth muscle caldesmon isoform (h-Cad)	Split Xiphoid of sternum, Exomphalos	Actomyosin and calmodulin binding protein, potential regulator of acto-myosin function. 97% penetrance of both phenotypes. Proposed mechanism: mechanical disruption due to changes in actomyosin contractility of smooth muscle cells within VBW or gut mesentery. Abdominal muscle layers present but hypoplastic.[160,161]
***Non-muscle myosin heavy chain II* (NMHCII) *Myh10* (*non-muscle myosin heavy chain B*)**	PC spectrum	Heavy chain sub-unit of non-muscle myosin II (NMHCII) protein. Roles in cell-adhesion, cell divisions, migration and actin cytoskeleton. Myh9 (heavy chain subunit A) and Myh10 expressed at leading edge SBW at E14.5. Model: Knock-in of motor impaired Myh10 is a dominant-negative gain-of-function interfering with both Myh9 and Myh10 function. PoC spectrum: Exomphalos (100%), ectopia cordis (50%) or split sternum, diaphragmatic hernia and cardiac defects.[162,163] *Myh10* null mice do not have VBW phenotype.[164] See Sections 4.2.5 and 6.1.

TABLE 2 (Continued)

Disrupted gene/ pathway	VBW phenotype	Gene/pathway information and mechanisms
ROCK1/ROCK2	Exomphalos	Serine/threonine protein kinases which regulate NMII contraction and the formation of supracellular actin cables. Functions downstream of planar cell polarity pathways. *ROCK1* and *ROCK2* expressed in VBW.[165] Proposed mechanism: Disruption of ROCK-dependent contraction of supracellular actin surrounding the umbilical ring. ROCK1 can compensate for ROCK2 and *vice versa*.[44,165,166] Also see Section 4.2.5.
Specc1l	Exomphalos	Associates with actin and microtubules. Binds NMIIB. Phenotype observed in gain of function mouse models which express mutated forms of Specc1L (in frame deletions) but not in mouse models which totally lack Specc1L expression (null or out of frame deletions). Altered actin-cytoskeletal distribution. Actin cables not formed appropriately in ectoderm at E13.5.[167]
Shroom	GS	F-Actin binding protein. *Shroom* is expressed in the somitic mesoderm and PBW at E10.5.[168] See Section 6.3.
Nuak1 (***Omphk1***)	Exomphalos, complete failure of SBW development	Serine/threonine protein kinase, which modulates actinocytoskeleton and inhibits Tgfβ signaling.[169] *Nuak1* expression at E9.5 in PBW, also expressed later in epidermis, sternal and abdominal bands.[170,171]
Inhibitory Neurotransmitter system		
Gad1/Gad2	Exomphalos	Glutamate decarboxylase (GAD), GABA synthesizing enzyme. Two isoforms: GAD67 is encoded by *Gad1* producing 90% GABA during embryonic development, and GAD65 encoded by *Gad2*. 100% penetrance *Gad1/Gad2* double knockout. Proposed mechanism: increased pressure within thoracic and abdominal cavity as a consequence of hunched posture of mice and/or increased abdominal muscle contractions but a review of GABA function in the gating of chloride channels suggests the GABA pathway may also play a role in tissue growth and tissue movement.[172–176]
VGAT	Exomphalos	Vesicular GABA transporter (VGAT) transports GABA and Glycine into synaptic vesicles. 100% penetrant.[172,174,177]
KCC2	Exomphalos	Neuronal-specific Potassium-chloride cotransporter, establishes chloride ion gradients necessary for GABA/glycine neurofunction.[178]

Note: Classification of VBW phenotypes: assessment of published reports on the mouse mutants linked to an interpretation of human VBW pathology. Full details of mouse mutants and phenotypes can be found in supplementary table. VBW is ventral body wall, LPM is lateral plate mesoderm, SBW is secondary body wall, PBW is primary body wall. Mutant phenotypes have been interpreted based on human VBW pathologies, definitions are outlined below. In the majority of mouse mutants, the phenotypes are not fully penetrant. Where a phenotype is fully penetrant, this is stated in the table. **TAS**; Thoracoabdominoschisis, defined here as fully open VBW with internal organs floating in amnion due to lack of a membrane cover. **PoC**; Pentralogy-of-Cantrell like, defined here as including fully open VBW with a membrane cover (ectopia cordis and omphalocele) together with anterior diaphragmatic hernia, anomaly of pericardium and structural cardiac defects. **LBWC**; limb–body-wall complex, defined here as open ventral body wall (with or without amnion cover) with truncated limbs. **Split sternum**: defined as failure of sternal bands to close and/or fuse. **Split Xiphoid of sternum**; bifurcation of the xiphoid process (the caudal part of the sternum). **GS**; gastroschisis, defined here as intestine floating in amnion or sitting in exo-coelomic space. **Exomphalos;** defined here as liver/intestinal herniation through the umbilical ring maintained after E16.5, with amnion covering. **BE** and **BE-like**: bladder exstrophy, BE; defined here as an open ventral bladder muscle wall and VBW into the amnion, BE-like; where the bladder muscular wall is closed but there is a deficient caudal ventral mesenchyme and body wall cover overlying the bladder. **Pubic diastasis**; separation of pubic bones of the pelvis. **PUH**: Physiological umbilical hernia. Also see Mouse Genome Informatics (MGI) website (https://www.informatics.jax.org/phenotypes.shtml) and International Mouse Phenotyping Consortium (IMPC) (https://www.mousephenotype.org/). Mutants of interest identified from website searches not included in Table 2 include the long noncoding RNA, *Fendrr*,[179] NFkB regulator, *IKK*,[180] serine protease, *Pcsk5*,[181] two regulators of the HH pathway in cilia, *Cp110* and *Ift25*,[182,183] the Filamin A interacting protein, *Luzp1*[184] and the aminomethyltranferase, *Amt*, which functions in mitochondrial folate metabolism.[185] Details of these mutants can be found in the supplementary table.

TABLE 3 Chromosomal abnormalities, gene associations, and human syndromes with VBW defects.

Chromosomal region	Human syndrome	Clinical presentation and gene association	Mouse mutant models	Reference
1p31.3 duplication		Exomphalos ***ROR1*, *FOXD3*, *ALG6*, *ITGB3*, *DLEU2L***	*Ror1*$^{-/-}$/*Ror2*$^{-/-}$	128,129,185
3q26.31-q29 duplication	3q duplication syndrome OMIM:611936	Exomphalos ***CLDN1*** and ***CLDN16*** (CLAUDIN-1/CLAUDIN-16), ***EPHB3*** Often associated with second chromosomal imbalance, for example, 9q34.3[186]	*EphB2/3* double knockout	17,104,186–188
11p15.5 deletion	Beckwith-Wiedemann Syndrome (BWS) OMIM: 130650	Exomphalos, prune belly ***CDKN1C* (*p57KIP2*)** has preferential maternal expression. *CDKN1C* germline mutation is associated with increased incidence of exomphalos in BWS patients. Epigenetic silencing of *CDKN1C* also implicated. ***IGF2***: variable loss of imprinting or hypermethylation	*IGF2* over-expression *p57kip2*$^{-/-}$ Caspary et al, 1999[189] reported a mouse model with *p57kip2* mutation and loss of *IGF* imprinting	108,157,189–193
Trisomy chromosome 13	Patau Syndrome OMIM: 264480	Exomphalos, bladder exstrophy		194–197
17p13.3 deletion	Miller–Diecker Syndrome OMIM: 247200	Exomphalos **HIC1** located within the 350 kb critical region for Miller–Diecker Syndrome	*Hic1*$^{-/-}$	70,73,198
Trisomy chromosome 18	Edwards Syndrome OMIM: 601161	Exomphalos		196,197,199
18q21.3		Exomphalos, ano-rectal malformation ***PIGN*** within a 20.43 Mb duplication. *PIGN* mutations are also associated with Fryn's Syndrome characterized by congenital diaphragmatic hernia (CDH).[200]		200,201
19p13.3	Cardio-facio-cutaneous Syndrome 4 OMIM: 615280	Exomphalos ***MAP2K2*** within a 1.27 Mb deletion. Belongs to group of RASopathies, germline mutations in Ras/MAPK signaling pathway. Clinically related Noonan Syndrome (OMIM: 163950), mutation in *PTPN11* also reported in patient with exomphalos.[202]	*Mesenchyme-cre Mek1*$^{-/-}$/*Mek2*$^{-/-}$	154,202,203
Trisomy chromosome 21		Exomphalos Reduced incidence compared to Trisomy 13 and 18, some studies suggest no association of exomphalos with Down's syndrome.[204]		204,205
45, X	Turner Syndrome OMIM: 309590	Exomphalos 5.1% of patients with 45,X karyotype ($n = 680$).		206,207
47XXY	KlineFelter Syndrome Focal Dermal Hypoplasia: Goltz-Gorlin Syndrome OMIM: 305600	Exomphalos, covered bladder exstrophy ***PORCN***.	Porcn$^{-/-}$	118,205,208,209

TABLE 3 (Continued)

Gene	Human syndrome	Clinical presentation and gene mutations	Mouse mutant	Reference
ALX4	Bladder exstrophy-epispadias complex (BEEC)	Bladder exstrophy 41 distinct *ALX4* heterozygous missense variants from 7500 patients analyzed.	*Alx4*$^{LstJ/LstJ}$	51,210
FILAMIN A (FLNA)	Otopalatodigital (OPD) spectrum disorder, OMIM:311300 OPD2, OMIM: 304120 Melnick-Needles Syndrome (MNS) OMIM: 309350	Exomphalos and prune belly *FLNA* mutations reported for all *OPD1* cases and 70% *OPD2*. *OPD2* associated with gain-of-function *FLNA* mutations. X-linked, with males exhibiting the most severe exomphalos phenotypes. Four males with mutations in *FLNA* presented with Prune Belly	*Dilp2* ENU mutation, males exhibit exomphalos.	146,211–215
FREM1	Manitoba-oculo-tricho-anal (MOTA) syndrome OMIM: 248450	Exomphalos Syndrome first described in patients of Aboriginal origin in Manitoba. Identical deletions of *FREM1* were identified in families from two patients.	*Frem1* $^{bat/bat}$ does not exhibit exomphalos.	216,217
GAD1		Wider and shorter thorax, exomphalos, rectal diastasis Exomphalos: Two siblings with bi-allelic loss-of-function mutations in the *GAD1* gene, one sibling also presented with a wider and shorter thorax. Rectal diastasis: One patient with a homozygous mutation in *GAD1*, from a cohort of six families. Study of Neuray et al.,[218] however, found no ventral body wall defects in six individuals with bi-allelic *GAD1* mutations.	*Gad1*$^{-/-}$ *Gad1*$^{-/-}$/*Gad2*$^{-/-}$ *VGAT*$^{-/-}$	172,218,219
ISL1	Bladder exstrophy-epispadias complex (BEEC)	Bladder exstrophy		220,221
LRP2 (LDLR2)	Donnai Barrow Syndrome OMIM: 222448	Exomphalos 50–70% of DBS patients exhibit exomphalos Two studies associate mutations in *LRP2* with exomphalos		222,223
PORCN	Focal Dermal Hypoplasia OMIM: 305600 aka Goltz-Gorlin Syndrome	Pentralogy of Cantrell (PoC), ectopia cordis, abdominal wall defect 71 disease-associated mutations in *PORCN*. 90% patients are female thus X-linked transmission.[224] PoC reported in three affected individuals. Ectopia cordis reported in two affected individuals. Abdominal wall defect reported in two affected individuals.	*Porcn*$^{-/-}$	118,224–227
PITX2	Axenfeld-Rieger Syndrome OMIM: 601499	Exomphalos >40% of ARS patients found with mutations in *PITX2*, exomphalos presents in 4.3% of RS patients.	*Pitx2* deficient mice	228,229
SPECC1L	Opitz G/BBB Syndrome type 2, OMIM: 145410 Teebi hypertelorism Syndrome, OMIM: 145420	Exomphalos One patient of two presented with exomphalos. 1 patient of 16 presented with exomphalos, 3 with an umbilical hernia. One patient of two presented with an umbilical hernia	*Specc1l*$^{CCD2/CCD2}$	167,230–233

(Continues)

TABLE 3 (Continued)

Clinical presentation	Human syndrome(s)	Comments	Potential mouse model	Reference
Fully open ventral (anterior) body wall with or without cover Exomphalos	Thoraco-abdominal Syndrome Pentralogy of Cantrell OMIM: 313850 Fryns Syndrome OMIM: 229850 Gershoni-Baruch Syndrome OMIM: 609545 Lethal omphalocele-cleft palate syndrome OMIM: 258320 VACTERL syndrome OMIM: 192350 V (vertebral anomalies), A (anal atresia), C (congenital heart disease), TE (tracheoesophageal fistula or esophageal atresia), R (reno-urinary anomalies), and L (radial limb defect). Shprintzen-Goldberg Exomphalos Syndrome OMIM: 182210	Linked to chromosomal abnormalities of Xq25-q27. Exomphalos observed sufficiently frequently in study of 524 infants with VACTERL syndrome it was proposed as an extended clinical presentation. Review by Kim, Kim, and Hui (2001)[234] implicate SHH signaling in this syndrome. Two of four family members presented with exomphalos and supported by a further patient study. Also linked to microdeletions in chromosome 22q11.[235]	*Tfap2α* null/chimeric mice, Transgelin cre- *Tgfr*β2 null (see Table 2) *EphB/EphrinB* Mutants *SHH/Gli3/Alx4* mutants (see Table 2) *Pcsk5* null (see supplementary table)	56,58,97,99,236 102,181,234,237,238 235,239–242
Multiple	Limb–body wall complex (LBWC), pentalogy of Cantrell (POC), Exomphalos exstrophy-imperforate anus-spinal defects (OEIS) complex, vertebral-anal-cardiac-tracheoesophageal fistula-renal-limb (VACTERL) association	**Nicotinamide adenine dinucleotide (NAD)** is a cofactor for ATP production in cells and a substrate for enzymatic reactions in metabolism, generated by tryptophan amino acid catabolism or dietary niacin metabolism. Deficiency of NAD in its oxidized form (NAD+) is proposed to be associated with multiple human syndromes. *Haao* gene is involved in metabolism of NAD+	Loss of function of *Haao* gene, dietary restriction of tryptophan and niacin led to exomphalos and gastroschisis in mice.	243,244

Note: Mouse mutant models are included where relevant, for further details, see Table 2 and supplementary table.

are molecular differences. As a consequence, abdominal versus thoracic VBW closure is differentially affected by different gene mutations (see Tables 2 and 3). Closure of the abdominal and thoracic VBW also can occur independently.

3.7 | Cell movements and body wall closure

Growth of the SBW is predominantly ventrally but there is also expansion in the thickness of the body wall at the midline and expansion along the cranial-caudal axes. Cell rearrangements and migrations contribute to differential growth along these axes. Analysis of cell behaviors in the embryonic mouse thorax at E12.5 reveals that presumptive sternal cells, which are located at the leading edge of the SBW (within the sternal band, see Figure 2A and Section 4.2.2), are preferentially orientated along the cranial-caudal axis and show no polarity, that is, cell protrusions are randomly oriented.[8] However, by E13.5, the orientation of the cell long axis has changed: now cells are orientated horizontally across the dorso-ventral axis. Live imaging of VBW explants has shown that there is cell intercalation across the dorso-ventral axis which narrows the presumptive sternum while increasing sternal dimensions along the other two axes.[8] These cell intercalation movements which change the shape of a tissue are known as convergent-extension and in the sternal mesenchyme are controlled by the protocadherins, Fat4, and Dchs1. In *Fat4* and *Dchs1* mutants, these cell movements fail to occur and the sternum is wider, thinner and shorter.[8] Similar patterns of cell movement have been observed for myofibroblasts at the leading edge of the thoracic and abdominal SBW.[99] Whether convergent-extension movements occur in regions other than the leading edge of the developing SBW, and/or within the PBW, is unknown.

There is also significant growth along the cranial-caudal axis, together with midline merging, of the infra-umbilical region. At CS17 (6 weeks) of human development, the UR and cloacal membrane are adjacent but from CS18 to week 9 a burst of cranial-caudal oriented growth dramatically separates the two.[245,246] This is linked to descent of the abdominal muscles such that both their cranial and caudal attachments move caudally. The oblique abdominal muscles also shift medially.[246] These authors also report the descent of the sternum at around the same time, which may reflect a broad caudal movement of the VBW as the lower abdomen grows. In mice, fate labeling and extirpation studies have demonstrated a similar caudal movement of infra-umbilical mesoderm at E12 which contributes to growth of the VBW and the dorsal genital tubercle (GT).[50] In a mouse mutant (*Alx4*$^{Lst/Lst}$) where this cell migration is defective, the GT is hypoplastic by E11.5.[50] This indicates that this caudal migration must start earlier before E11.5. As well as growth along the cranial-caudal axis, these cell movements are also linked with the merging of paired genital swellings. The two genital swellings are generated from the LPM and are initially located on each side of the cloacal membrane following embryonic folding.[247,248] Subsequently, the two genital swellings merge at the midline to overlie the cloaca. Signals from the cloaca, such as Fgf and Shh, also control development of the genitalia.[248–252] The physical proximity, the shared morphogenetic processes and signaling interactions explain why caudal VBW anomalies such as bladder and cloacal exstrophy (CE) are often associated with genital anomalies (see Sections 5.2.5 and 6.5).

There is also additional evidence of considerable cell movement along the cranial-caudal axis at the midline. DiI labeling of the thoracic LPM in stage 20 chick embryos (equivalent to E10.5 mouse embryos) shows that LPM expands along the cranial-caudal axis and by day 10 the labeled cells are located as a line along the fused ventral midline of the embryo.[19] How this extensive cell movement is directed is unknown.

4 | MOLECULAR REGULATION OF VBW CLOSURE

Several signaling pathways and cellular processes have been identified as being essential within the PBW or SBW for VBW closure. Amongst these are the Tgfβ, canonical Wnt, Rho/ROCK signaling pathways and the transcription factors, Tfap2α and Six5/6. Six5/6 is essential within the PBW while Tgfβ and the canonical Wnt signaling pathways are required for SBW closure (β-catenin and Wnt signaling references in Table 2). Pitx2 and Tfap2α are required for both PBW and SBW development.[56,80,81,253] These pathways control cell proliferation, survival, migration, differential cell adhesion and differentiation. ROCK signaling, which regulates the actin cytoskeleton and presumably, cell and tissue mechanics, appears necessary for the final step of body wall closure. Additionally, there are collective organized cell behaviors which change the relative dimensions of the thoracic body wall and are determined by the planar cell polarity (PCP) pathway, Fat4/Dchs1, as previously discussed (Section 3.7). The better characterized signaling pathways involved in VBW closure are discussed below and in Section 6. Additional genes that are essential for VBW closure are listed in Table 2 together with information about their potential roles, where known. Additional

information about the mouse mutants and their phenotypes is also presented in Table S1.

In the following section, PBW formation will be discussed (Section 4.1) followed by consideration of how signals from the PBW influence SBW formation and molecular mechanisms of SBW development (Section 4.2).

4.1 | Formation of the PBW

Understanding the folding of the early LPM forms the basis of understanding PBW development. This folding initially requires the co-ordinated interdependent morphogenesis of the LPM (somatopleure, splanchopleure), endoderm together with the extra-embryonic tissues which must move together (Figure 1A). During the later phase of VBW closure, the somatopleure that will form the PBW develops independently of the splanchopleure (Figure 1C). In the mouse, folding starts cranial-caudally at the AIP at approximately E8 (Figure 1A). VBW defects due to abnormal PBW development may arise by failure in folding and development of the PBW due to defective development of one of the PBW tissue layers (see below). Alternatively, VBW defects may arise due to an alteration in signals from the PBW that affect SBW development (e.g., Tgfβ2, see Sections 4.2.1 and 4.2.3). In mice, phenotypes that are due to defective development of the PBW will be apparent by E11.5. Phenotypes due to defective signaling from the PBW will be apparent later. In the following section, we discuss key genes that are essential for different phases of PBW development in mouse embryos.

One of the first transcription factors seen in the LPM around the timing of embryonic turning at E7.5/E8.5 is the zinc finger transcription factor Gata4. There are particularly high levels of *Gata4* expression in and around the AIP.[254–257] Within these domains, Gata4 transcriptionally activates *Bmp4* expression in the LPM, which in turn positively regulates *Gata4* expression.[258,259] Lineage tracing experiments have confirmed that LPM cells in the PBW are derived from the early Gata4 expressing cells.[254,257,260] *Gata4* null mice arrest development around the time of ventral folding with the defect apparent by E8. This model clearly shows failure of the LPM to fold ventrally, such that the embryo grows outside the yolk sac.[256] Chimeric embryos made with *Gata4* null and *Gata4*-expressing cells have indicated that Gata4 function in the endoderm, but not the LPM, is essential for ventral folding.[261] This conclusion is also supported by specific deletion of Gata4 in the LPM. In these mice, the PBW forms but is thinner by E13.5.[254] As Gata4 is only transiently expressed in the somatopleure up to E8.5, this must reflect an early role of Gata4 during establishment of the PBW.[257]

The *Gata4* null mouse resembles the *Furin* null mouse where there is also arrested cranial-caudal and lateral folding which is clearly apparent by E8.5.[107] In *Furin* null embryos, an additional phenotype has been reported in the allantois which is highly vacuolated and fails to fuse with the chorion.[107] Furin is an intracellular processing protein which is also expressed in the AIP, LPM and extra-embryonic tissues at E7.5 to E8.5. One of the roles of Furin is to cleave and activate Tgfβ family members, including Bmp4.[262] However, despite the resemblance of the *Gata4* and *Furin* null embryos, the phenotype is not the result of loss of Gata4 as a secondary consequence of decreased Bmp signaling. In *Furin* null mice, *Gata4* expression is only absent is in the allantois but other domains of *Gata4* expression persist.[107]

The basic helix–loop–helix transcription factors, *Hand1* and *Hand2*, are highly expressed in the LPM and also extraembryonic tissues between E7.5 and E9.0.[263–266] In the post-turning embryo *Hand1* and *Hand2* expression in the VBW is largely lost, with *Hand1* expression becoming confined to the umbilical cord region by E11.5.[263–265] Lineage tracing experiments have confirmed the Hand1-expressing cells give rise to the PBW.[69,263] Embryos null for *Hand1* or *Hand2* fail to complete the folding process, and arrest development by E9.5 with a phenotype where the PBW does not form and the VBW is open, resembling TAS VBW anomaly. Selective deletion of *Hand1* in the LPM results in a spectrum of VBW phenotypes ranging from an enlarged UR in pups to a gastroschisis (GS) type of VBW anomaly with the herniating gut right of the umbilical cord, lacking any tissue cover.[69] This indicates that expression of Hand1 within the extra-embryonic membranes may be essential for embryonic folding while expression within the LPM is needed for later closure events.[69]

Loss of the paired-homeodomain transcription factor *Pitx2* can also disrupt early turning in some embryos.[80,81,228,253] However, in all embryos, Pitx2 is essential to establish the appropriate geometry of the somatopleure once folding has started. In *Pitx2* mutants, the left forming part of the VBW is bent outward, instead of bending medially toward the opposing right body wall at E9.5.[80] The left LPM and adjacent amnion are also thickened, possibly mechanically restricting bending.[80] This asymmetric anomaly presumably reflects the asymmetric expression of *Pitx2* within the early LPM.[79,80,116] Analysis of the LPM in E10.5 *Pitx2* mutants has identified loss of the expression of some members of *Hox* (9, 10, 11 paralog groups) and *Tbx* family members (Tbx4, -15), while expression of other *Tbx* genes is either increased (Tbx6) or they are ectopically expressed (Tbx1, -2, -5).[82,83] Hox and Tbx genes determine regional identity of cells within an embryo indicating that the specification of the

LPM has been disrupted. *Pitx2* is a transcriptional target of canonical Wnt signaling and in turn, there are also changes in the levels of components of the canonical and Wnt PCP pathways which would be predicted to alter cell proliferation/survival and co-ordinated cell behaviors, respectively.[82–84,267]

The sine oculis homeobox transcription factors 4 (Six4) and 5 (Six5) show expression in all three layers of the PBW where they play key roles in each layer: ectoderm, mesoderm, and coelomic epithelium. *Six4*$^{-/-}$; *Six5*$^{-/-}$ mice show a remarkable "pure" exomphalos anomaly, the thoracic midline closes completely and portions of the liver and intestine can be seen herniating through the VBW covered by a thin sac that has the umbilical cord at its center.[86] In this double mouse mutant, the anomalies in the PBW appear at approximately E9.5 of development and are restricted to the abdominal VBW.[86] There appears to a general failure to narrow the UR which is linked to an accumulation of cells at the lateral edge of the UR, together with decreased proliferation and increased apoptosis in the ectoderm and mesoderm at the lateral edges of the PBW.[86] Additionally, differences in the morphology of the coelomic epithelium have been observed in *Six4/5* double mutants. Overexpression of Six4 within the coelomic epithelium promotes epithelial-mesenchymal transition (EMT) suggesting that Six4 and 5 may also regulate EMT and contribute to thickening of the body wall.[86] The selective restriction of the defect to the periumbilical region and the normal closure of the thoracic midline suggest that Six4/5 are required in differential growth of the right and left hemi body walls in a restricted region in the abdomen rather than being essential in the development of the whole PBW.

In summary folding of embryo to form the PBW requires the transcription factors, Gata4, Hand1/2, Pitx2, and the metalloproteinase furin1.[56,79–81,107,116,253,255,256,264] As the PBW is being generated, there are cell migrations that contribute to the thickening of the PBW. These cell migrations do not occur appropriately in *Tfap2α*, *Pitx2*, and *Six4/5* mouse mutants resulting in either a failure to close the PBW (Pitx2) or a thinner PBW which is vulnerable to rupture (Tfap2α), or contributes to a failure to close the SBW (Six4/5).[56,80,86]

At E9.5/E10 in the mouse, the PBW is demarcated from the forming SBW by the transcription factors Agouti, Alx3/4, Msx1/2, Hand1/2, Pitx2, Six5/6, and Tbx5.[38,51,74,77,79,86,92,263,268] The PBW provides a physical and signaling framework upon which the fully differentiated VBW will be established by infiltration of cells from the SBW (Figure 2A–C). The ultimate fate of the PBW needs to be resolved. Chen et al. reported degeneration of the PBW as the SBW invades.[269,270] However, the persistence of a thin membranous cover, in many mouse mutants, where there is a failure of SBW formation (e.g. *Tgfβ*, see Table 2) indicates at least part of the PBW may normally persist.

4.2 | The SBW

4.2.1 | Signals from the PBW control SBW development

Signals from the midline control development of the SBW (Figure 2A). First, signals from the LPM, including Bmp4, help establish the hypaxial musculature, and timing of differentiation, within the early somite.[271,272] Subsequently, myotomal extension is controlled by Wnt signaling from the PBW (together with signals from the SBW ectoderm).[39,116] Tgfβ signaling from the PBW ectoderm is also required for function of myofibroblasts, a critical cell population within the closing body wall[99] (and see Sections 4.2.2 and 4.2.3). In the chick, Bmp signals from the PBW ectoderm and mesoderm also control rib extension.[18]

4.2.2 | The leading edge of the SBW is essential for VBW closure and is unique

In the thoracic VBW, the ventral edge of the SBW is demarcated by a band of *Sox9*, *Runx1 & 2*, *Tbx5* and *ephrinB1/B2* expression which in mice probably demarcates all the LPM (Figure 2A–C).[4,19,102,104] This is histologically visible as a denser group of cells at E12 and has been termed the developing sternal band.[273] This domain moves ventrally as the SBW expands (Figure 2A–C). *Tbx* gene family members (*Tbx1*, *-2*, *-4*, *-5*, *-6*, and *-15*), *Hic1* and *ephrin B1/B2* also demarcate the leading ventral edge of the abdominal SBW and this domain is known as the abdominal band and is a subdivision of the LPM (Figure 2C).[73,84,102,104] These ventral leading edges consist of a heterogeneous cell population of different cell origins which includes myofibroblasts and are associated with the cutaneous nerves.[35,99] Based on their histological spatial relationship ahead of other differentiating components of the VBW, the sternal and abdominal bands are proposed to be critical regulators of VBW closure.[20,26,35] Indeed, some of the genes (*Runx1/2*, *Hic1*, *ephrin B1/B2*) within this leading edge are essential for VBW closure (Figure 2A,C; Tables 2 and S1). The myofibroblasts within this domain are also essential for body wall closure[99] (and see Section 4.2.3). *Tfap2α* is highly expressed in the ectoderm overlying these mesenchymal domains (Figure 2C).[56] Curiously, histological analysis has shown that the abdominal

band, and associated cutaneous nerves, are absent in *Tfap2α* mutants which are characterized by an open body wall with disorganized connective tissue and delayed muscle differentiation.[56]

4.2.3 | TGF-beta signaling and the role of myofibroblasts

Aldeiri et al. reported a migrating population of Transgelin (Tagln, also known as SM22α)-expressing myofibroblasts within the thoracic and abdominal VBW.[99,100] The myofibroblasts appear in the dorsal body wall by E10.5 and then advance toward the ventral midline. By E11.5, they fill the breadth of the PBW and are also found at the leading edge of the SBW ahead of the developing sternum, ribs, and hypaxial musculature.[99] By E15.5, they are positioned at the ventral midline, staying in this location into the post-natal period.[99] These are presumably the same cells as the αSMA populations identified between the two opposing sternal bars as they meet at the midline at E14.5.[49] Aldeiri et al. proposed that they are a pioneering cell population instrumental for VBW closure.[99] Whether myofibroblasts function by paracrine signaling to adjacent tissues or act mechanically is still unclear.

The myofibroblasts express Tgfβr2 and migrate ventrally in response to Tgfβ2 from the PBW ectoderm (Figure 2A).[99] Conditional inactivation of Tgfβr2 within the Tagln-expressing cells (but not myogenic or chondrogenic cells) results in a Pentalogy of Cantrell (PC) phenotype which is characterized, in part, by the failure to close both the thoracic and abdominal VBW (see Section 6.1). This clearly demonstrates that Tgfβr2 signaling within the myofibroblasts is essential for VBW closure.[99,100] However, the phenotype does not include bladder exstrophy indicating there are different cellular and/or molecular mechanisms of closure of the lower (caudal) abdominal VBW. It is currently unclear if this population of cells is the same or includes the population of invading "undifferentiated spindle-shaped cells" identified at the forefront, that is, leading edge of the SBW in both mouse and chick embryos.[20,269,270] Chen hypothesized that this cell population drives VBW closure and demonstrated that the leading edge of the SBW is able to close in an ex-vivo explant culture in the absence of adjacent tissues.[26] The Tagln migratory fibroblasts have been proposed to arise from the somite and might also overlap with the somite (sclerotome and syndetome) derived *Hic1*-expressing cells.[72] *Hic1* expressing cells are found at the leading edge of the SBW, spatially overlapping with Tagln (Figure 2C).[70,72,99] *HIC1* is deleted in Miller-Dieker Syndrome, a contiguous gene disorder, where exomphalos can occur (OMIM 247200). Moreover, the *Hic1*$^{-/-}$ mouse mutant can exhibit exomphalos, although this phenotype is not fully penetrant.[73]

4.2.4 | The Wnt pathways are key regulators of SBW closure

Wnt signaling in both the ectoderm and mesenchyme is required for appropriate VBW closure.[49,116,117] Wnt signaling includes a canonical pathway, which controls cell proliferation, survival or differentiation, and PCP pathway components which control co-ordinated cellular behaviors or cellular characteristics across a plane of tissue.[274,275] Core components of the canonical pathway include the transmembrane proteins, LRP5/6 and the intracellular effector molecule, β-catenin. The Wnt-PCP pathway includes Vangl1/2, Ror1/Ror, and Ryk proteins. Loss of function of both canonical and Wnt-PCP components result in VBW closure anomalies highlighting the crucial role of both branches of the Wnt signaling network. Defects in Wnt signaling include open thoracic and abdominal VBWs, a thin tissue layer at the midline, and a split sternum.[39,49,116,117]

Analysis of canonical Wnt reporter mice shows that canonical Wnt signaling is active within the midline of the VBW (Figure 2A).[39,49] In mouse embryos, following mesenchymal inactivation of β-catenin or of LRP5/LRP6 co-receptors, critical components of canonical Wnt signaling, the midline of the VBW remains thin and appears not to be populated by the SBW.[39,49] This phenotype can be explained by the three roles of β-catenin within the VBW mesenchyme: survival, proliferation of mesenchymal cells and differentiation of the dermal fibroblasts.[39,40] Additionally, canonical Wnt signaling controls migration of the myogenic cells into the VBW.[116] A transcriptional target of canonical Wnt signaling in both the mesoderm and developing musculature is Pitx2, also essential for VBW closure and muscle development[84,267] (see Section 4.1).

Wnt5a and *Wnt11*, which are typically linked with PCP pathway components are expressed in the VBW mesenchyme.[49] In *Wnt5a* mouse mutants the thoracic VBW remains open while *Ryk*$^{-/-}$ */Vangl2*$^{-/-}$ and *Ror1*$^{-/-}$/*Ror2*$^{-/-}$ double mutants are characterized by exomphalos, where the abdominal VBW has not closed appropriately, and a lack of growth of the lower abdomen.[127,128] Coupled with limb anomalies, this phenotypic spectrum resembles limb–body wall complex (LBWC) (see Section 6.1). Based on the pathways function in other tissues,[274] the Wnt PCP pathway is predicted to regulate convergent-extension and oriented cell divisions but this has not yet been demonstrated in the VBW. Loss of Wnt-PCP signaling results in a decreased rate of migration

and ectopic exposure of Wnt5a increases cell migration suggesting Wnt5a may control collective cell migrations/movements in vivo.[49]

4.2.5 | Mechanical forces may pull the SBW closed

Mechanical forces include tensions and forces from neighboring cells and the matrix environment which acting together can influence cell behaviors such as orientated cell divisions, migratory behaviors and cell intercalations in addition to cell differentiation. For example, myofibroblast migration will be determined by mechanical factors, such as matrix organization and stiffness, in addition to chemotactic cues. Alterations in the matrix organization, and presumably stiffness/tension are also linked to VBW anomalies as illustrated by the *Bmp1*, *glucocorticoid receptor*, and *Alcp* mutants (see Tables 2 and S1). Intracellularly, these mechanical forces are mediated by alterations in the actin cytoskeleton via alterations in the activity of ROCK kinases and non-muscle myosins, together with changes in transcriptional responses mediated, via, for example, Yap/Taz, canonical Wnt, and EGR pathways. Candidate intracellular mechano-effectors that have a VBW phenotype when mutated are listed in the "cytoskeletal components" in Table 2. For example, loss of the actin cytoskeleton, through inhibition of ROCK, would decrease the ability of cells to respond to mechanical cues. *ROCK1*$^{-/-}$ and *ROCK2*$^{-/-}$ mouse mutants are characterized by exomphalos but the penetrance of the phenotype is dependent on genetic background,[44,165,166,276] In wild-type E16.5 embryos, filamentous actin is present at the UR, a region of thickened ectoderm between the body wall ectoderm and amnion. In *ROCK1*$^{-/-}$ mutants, this thickened ridge of ectoderm is absent and there is decreased actin staining.[44] As the actin cytoskeleton responds to, and can drive, mechanical changes this suggests that the actin cytoskeleton narrows and closes the umbilicus. Chemical inhibition of ROCK activity in early chick embryos at the stage of PBW formation results in body wall defects but the precise role of mechanical forces, and the actin cytoskeleton at this early stage of development is unknown.[277] A mutation in non-muscle myosin heavy chain B (NMHCII-B^{R709C}; NMHCII-B also known as Myh10) that impairs motor activity results in VBW defects.[162,163] Again, as for other signaling components, there are differential sensitivities along the cranial-caudal axis. Heterozygous NMHCII-B^{R709C} mice have exomphalos while homozygous NMHCII-B^{R709C} mutant mice exhibit both thoracic and abdominal closure defects.[162,163]

5 | CLINICAL VARIANTS OF BODY WALL CLOSURE DEFECTS

5.1 | Introduction

The clinical correlates of the embryological pathophysiology so far described are imperfect but form a necessary translational aspect to the science. We will consider this with a detailed exploration of factors that have been implicated in the clinical condition and a brief description of the various conditions broadly encompassed by the term—abdominal wall defect (AWD).

5.2 | Clinical correlates

5.2.1 | Ectopia cordis

There are less than 100 cases in the literature[278] and it can be divided into two broad categories: those where only the heart protrudes from the thoracic cavity and those where it forms part of a more syndromic entity (e.g., PC, considered below). There is no apparent racial variation, and its incidence has been quoted at 5 per 10^6 births. Early antenatal diagnosis should be possible from the 12th week of gestation and the usual outcome would be elective termination. For those few carrying to term, a successful repair is seen to be much more likely in those forming part of a Cantrell syndrome. The first successful repair of an isolated ectopia cordis only occurred in the 1970s involving a staged process of initial skin flaps and later actual reduction into the thoracic cavity with fashioning of sternum and rib cover. There are very few long-term survivors though.

5.2.2 | Syndromic AWDs

The principle syndromic midline AWDs of PC, Thoracoabdominal Syndrome (TAS), and the LBWC can be considered together. Exomphalos (omphalocele), bladder and cloacal exstrophy, imperforate anus, spina bifida (OEIS) will be considered in a later section.

James Cantrell et al. from Baltimore described 5 cases and added 21 cases from the literature[279] of an association of five related anomalies (exomphalos, diaphragmatic defect, pericardial defect, sternal cleft, ectopic cordis [or intracardiac defects]) in 1958. Much of the subsequent literature has been based on case reports with some exceptions[280] so there is very little actual consistent evidence for causation. The only registry-based estimate of incidence is 1 in 200,000 live-born infants.[281]

One does not require all five components; indeed, the ectopia cordis element is now extraordinarily rare but at the very least there should be epigastric exomphalos, central diaphragmatic defect and perhaps absence of xiphisternum/cleft sternum. Genetic factors may be important in a few, with a number of trisomies reported (21, 18) as well as Turner Syndrome, with one report identifying concurrence with the Goltz-Gorlin syndrome (characteristic facies, anophthalmia, cleft lip and palate; limb malformations and dermal defects).[225] This latter condition has been linked to an X-linked (Xp11. 23) *PORCN* (Porcupine) mutation in almost all cases, that has an important role in mediating Wnt ligand palmitoylation[282,283] (see Section 6.1).

TAS (OMIM 313850) is characterized by X-linked midline defects that include diaphragmatic and ventral hernias, hypoplastic lungs, and cardiac anomalies and was first identified in an Israeli family[236] with the TAS gene mutation being mapped to the region of Xq25–q27.

LBWC is very rare and fatal (usually intrauterine, sometimes as a stillborn birth) with a wide range of phenotypic pathologies including exomphalos together with cranio-facial anomalies (exencephaly, encephalocele, facial clefts); and limb defects (e.g., talipes, absent limbs, oligodactyly, sometimes with features of amniotic bands).[284,285] There have been no defined genetic or predisposing factors, beyond a report relating two LBWC fetuses to heavy use of smoked crack cocaine in the mother.[286]

5.2.3 | Gastroschisis

GS is probably the commonest AWD and is very familiar to all pediatric surgeons. There is a full-thickness AWD almost always to the right of the normally-inserted umbilicus. It is an isolated defect in the vast majority and those associated anomalies are mostly caused by the actual defect itself (e.g., midgut deletion, gastrointestinal atresias, undescended testes).

The actual timing of the defect is not known with any certainty and its cause remains entirely speculative. One recent suggestion[287] is that the developing cord normally has two parts, a firm left-sided part formed by the vessels and urachus, and a thin right-sided pouch covering the intestinal loops (the "physiological umbilical hernia"), which is at risk of rupture. That is, this is a secondary event following completion of the abdominal wall occurring between 10 and 14 weeks gestation. There is then intestinal prolapse led by the midgut with increasing hernial ring dilatation. Nonetheless this ring can contract later pinching off the midgut and causing ischemic compromise and even total infarction—so-called "closed GS"—with devasting consequences.[288]

5.2.4 | Exomphalos (aka omphalocele)

Exomphalos may be defined by midline absence of abdominal wall fascial integrity but with preservation of a sac covering the protrusion of the intra-abdominal viscera. There is wide separation of the rectus muscles around the defect. Clinically we recognize a spectrum based on size of defect and intactness of sac but clinically categorize into Major (>5 cm diameter defect ± presence of liver within sac) and Minor (<5 cm diameter) with two smaller categories at either end—Giant (based more on size of sac rather than defect diameter) and the small "hernia-in-cord" which appears as a rather thickened insertion of the umbilicus and a visible bowel loop within. Umbilical hernias are post-natal in origin related to failure to complete the cicatrization process at the level of the insertion of the ligated umbilicus and will not be considered further.

Exomphalos (typically major) are associated with various trisomies (mainly 18, 13) and gene mutations consistent with the Beckwith-Wiedemann syndrome (BWS) (located on chromosome 11p15)[289] that have an association with exomphalos minor. Associated non-syndromic anomalies are not uncommon. The British Association of Pediatric Surgeons Congenital Anomaly Surveillance System reviewed all 162 infants with exomphalos born during the 2-year period March 2014 to February 2016 in the United Kingdom and Ireland. Most of these had other congenital anomalies and could be classified as syndromic (e.g., trisomy 18) ($n = 15$, 9%), other structural anomalies ($n = 72$, 44%) and the BMS ($n = 29$, 18%). Only 46 (28%) infants could be described as having an isolated exomphalos (personal communication). Furthermore, lung hypoplasia can be clinically important and relates to the size of the defect and negative impact of extra-abdominal viscera on the developing lungs.

5.2.5 | Classic bladder exstrophy, cloacal exstrophy (CE), and OEIS

Lower midline AWDs include **bladder exstrophy** and **CE** with the most severe defect along the spectrum being termed **OEIS complex** (OMIM 258040). Classic bladder exstrophy has a number of related features with failure of the ventral aspect of bladder and abdominal wall; a split pubic symphysis and divergent rami; and epispadias in boys. CE similarly has fusional failure of the lower abdominal wall with a small exomphalos above an opened out undifferentiated cloaca consisting of a central caecal plate with two template hemi-bladders on either side.[290] There is usually a prolapsed distal ileum giving a characteristic "elephant's trunk" appearance. A hindgut

orifice on the caecal plate leads to a blind anorectum. Genitalia in both sexes are invariably bifid and hypoplastic with vaginal duplication/agenesis and uterine duplication in girls and a bifid phallus and undescended intrabdominal testes in boys. Indeed, in 46XY boy's phallic structures may be so hypoplastic as to preclude anatomical and functional penile reconstruction leading to gender reassignment (certainly the historical preference). OEIS involving not only ventral but dorsal midline defects was first defined by Carey et al.[291] and with increasing appreciation of the degree of spinal involvement (dysraphism, tethered cord syndrome, myelomeningocele) nowadays is almost used synonymously with CE.[290] CE has an estimated incidence of about 1 in 130,000 births[194] with up to 20% of them having defined features of OEIS.

5.2.6 | Prune belly (aka Eagle Barrett syndrome, Prune Belly Association)

Prune belly syndrome (PBS) has been characterized by deficient or absent abdominal wall musculature, hypotonia, together with pathological dilatation of the urinary system and (in males) bilateral intra-abdominal testes (it rarely occurs in females). Its unusual name was coined by the Canadian physician William Osler in 1901 describing its most obvious abdominal wall appearance. Most present antenatally with hydronephrosis, a low-pressure distended bladder and oligohydramnios. Severe degrees of renal impairment and accompanying lung hypoplasia are poor prognostic features with perinatal mortality between 10 and 25%.

5.3 | Environmental/epidemiological aspects

The epidemiology and influence of environmental factors have only really been studied in the two principle AWDs of exomphalos and GS, the others being far too rare for consideration.

5.3.1 | Epidemiology of AWDs

Since the 1960s, the distinction between the GS and exomphalos (synonymous with omphalocele) had been recognized and while the prevalence of exomphalos has remained static (with caveats—see below) that of GS has been consistently rising at least in Western societies[292,293] although there may be some recent evidence of a leveling off.[294] The reasons for this remarkable observation are essentially unknown. So, the current incidence in the United Kingdom varies from 1 in 3000 to 1 in 8000 live births, with the higher values seen in urban industrial areas.[295] The incidence of exomphalos has plateaued since the 1970s, being 1 in 2600 in one large UK study (2005–2011)[296] with a mean maternal age at delivery being 29.2 years (same as controls). Certainly, by contrast, young maternal age does appear to be a significant factor in GS.[294,297] In one Californian study mothers <16 years of age had 4.2-times greater prevalence of GS than mothers between the ages of 25 and 29 years.[292]

Ethnicity, likewise, appears important with white Caucasians and native Americans having a higher risk of GS than either black or those of Hispanic origin in the United States.[292,297] Finally, lower household income or social group status may also have an effect in GS.[297]

The prevalence at birth of exomphalos, however, masks a considerable loss during intrauterine life. This is not only naturally, but also iatrogenically with the advent of almost universal screening maternal ultrasound and ability to define severe genetic abnormalities at increasingly earlier gestational ages. As an illustration of this, Lakasing et al.[298] from King's College Hospital, London reviewed the outcomes of 445 fetuses with exomphalos; 56% of which had a defined chromosomal anomaly, 30% had a normal karyotype (remainder not karyotyped due to parental request). Fetuses with chromosomal anomalies and other potentially severe anomalies were usually offered termination. Ultimately, 55 (18%) were actually live-born.

5.3.2 | Environmental factors

In general, these are more well-established albeit by no means proven for GS than for exomphalos.

Gastroschisis

There have been associations with maternal drug use both illegal (e.g., cocaine, heroin) and legal (e.g., aspirin, ibuprofen).[297] Most of these studies rely on self-administered questionnaires and recall, which clearly has its own limitations, but one study from Leicester, UK[299] used maternal hair analysis to verify and confirmed a link with vasoactive recreational drugs (e.g., Ecstasy, cocaine; OR = 3.3, 95% CI: 1.0, 10.53) and a very marked association with 1st trimester aspirin (OR = 20.4, 95% CI: 2.2, 191.5). Nevertheless, some recent population studies from California,[297] and London[300] have disputed this. The latter study used the same hair analysis technique and initially showed the same relationship for recreational drug use (25% vs. 13%) but the difference became less significant when corrected for maternal age (25%

vs. 21%). By contrast, the incidence in the exomphalos group was 7% throughout. There have been other environmental factors suggested as of significance in GS but most remain speculative. Thus, Torfs et al.[301] suggested that maternal occupational exposure to solvent use (e.g., paints, glues) had an association, though this did not stand up to analysis in a large study based on the National Birth Defects Prevention database.[302] Similarly, a small Welsh case–control study[303] suggested that a higher intake of fruits and vegetables during the first trimester and higher body fat percentage were associated with a reduced risk of GS and confirmed an earlier link with maternal smoking. Perhaps more contentiously, some studies have suggested an association with the use of some agricultural herbicides (specifically Atrazine).[304]

Exomphalos

Many studies have discriminated between syndromic and non-syndromic exomphalos implying more genetic issues in the former. So in a large American National Birth Defects Prevention Study[297] ($n = 168$ [non-syndromic], 4967 controls), infants tended to be male, arising as part of a multiple birth and less likely to be born to a multipara woman. Women were more likely to have consumed alcohol (OR = 1.53; 95% CI, 1.04–2.25), and to be heavy smokers (OR = 4.26; 95% CI, 1.58–11.52) than controls.

Atmospheric pollution has been suggested as a possible causative agent in the etiology of congenital anomalies[305] and, specifically sulfur dioxide pollution has been linked in one study from Liaoning Province, China[306] with a modest increased prevalence of exomphalos (OR = 1.39, 95% CI = 1.22–1.65).

6 | ANIMAL MODELS OF VBW DEFECTS AND RESEMBLANCE TO HUMAN PATHOLOGY

VBW anomalies can be caused by changes in a variety of cell behaviors, as outlined in Sections 2 and 3. These defects may occur during the initial folding of the somatopleure and splanchopleure, at the lateral, cranial and caudal edges, or during subsequent growth and morphogenesis of the VBW. Most of our knowledge on VBW closure, and the mechanisms that govern its anomalies, is derived from animal models of VBW closure defects. While these models provide insight into human pathology, it is inappropriate to draw exact parallels between the anomalies in mice and humans. The more severe forms of ventral closure defects encountered in human embryos are rarely an isolated pathology and are generally associated with other genetic or structural abnormalities. These cases do not survive to a live birth or undergo termination of pregnancy. Hence, the clinical phenotype is not well understood and it is estimated that at most 10% of embryos identified to have an AWD will survive to birth.[298] Hence, a viable human VBW pathology represents the milder forms of VBW closure defects in comparison to animal models. Nevertheless, the process of VBW closure is largely preserved in mammals, and animal models of closure defects provide a platform to study these anomalies in humans. This section will focus on animal models of VBW closure defects analyzed from a human pathology narrative. We will discuss key pathways that are linked to VBW closure anomalies in mice, crucial cellular and molecular mechanisms, and their relevance and representation in human pathology. The following discussion refers to mouse models unless stated otherwise. Additional animal models are listed in Table 2 (also see Table S1 for details of each mouse mutant and their phenotypes). Human gene associations and chromosomal changes frequently linked with clinical VBW pathologies are listed in Table 3.

6.1 | Syndromic AWDs

Exomphalos (omphalocele) is a known association in many human syndromes, the most common are BMS, trisomy 13 (Patau syndrome), trisomy 18 (Edwards syndrome), and PC. It is also reported, to a lesser extent, in focal dermal hypoplasia (FDH), Shprintzen Goldberg Syndrome, and many others. Animal models recapitulating some of these syndromes demonstrate a high degree of overlap in developmental phenotypes including VBW closure defects and are discussed below.

BWS is the most recognized human syndrome associated with exomphalos. Two specific genetic defects in the imprinting cluster regions 1 and 2 on chromosome 11p.15.5, lead to improper expression of different genes and result in BWS. These genes include IGF2 (insulin-like growth factor II), H19, KCNQ10T1 (LIT1), and CDKN1C (p57[KIP2]). The H19/IGF2 and CDKN1C/KCNQ1OT1 clusters and their regulatory mechanisms are conserved in the mouse and are located at distal chromosome 7.[307] Modeling BWS using a paternal uniparental disomy of chromosome 7 (PatDp(dist7)T9H-0/*Tg*) or in mice lacking the imprinted Cdk inhibitor $p57^{KIP2}$ resulted in VBW closure defect. These mutants display a spectrum of secondary VBW closure defects ranging from an exomphalos-like anomaly to a thinned ventral skin and musculature, together with other developmental elements resembling BWS in humans.[157,308]

PC is a constellation of ventral anomalies including the heart, diaphragm and the VBW. The exact etiology is unknown, and the majority of cases are sporadic. Genetic

clues to the pathogenesis of PC are implied in familial cases through chromosomal abnormalities, such as Turner Syndrome, and in some reports of FDH (Goltz-Gorlin syndrome).[225,226,236,281,309] The full phenotypic spectrum of PC is emulated in a number of mouse models targeting the Tgfβ pathway, homeobox genes and non-muscle myosin heavy chain type II (NMHCII encoded by the *Myh10* gene)[74,97,100,162,163,310] The Transgelin (Tagln)-Cre Tgfβr2 null mouse, in which Tgfβ is inactivated within a SBW leading edge myofibroblast population, recapitulates all aspects of PC. These mice are characterized by ectopia cordis, anterior diaphragmatic hernia, a single outflow tract (truncus arteriosus) and ventricular septal defect, an absence of the diaphragmatic pericardium and finally exomphalos.[100] The exact role(s) of Tgfβ signaling within the myofibroblasts is yet to be established. Similar constellation of the congenital defect can be observed when Homeobox genes are disturbed. The $Hoxb4^{PolII}$ homozygotes demonstrate ectopia cordis, failure of ventral abdominal wall closure, herniation of the liver to a thoracic position, failure of anterior pericardial sac formation and a varied spectrum of structural cardiac defects.[74] The defect in the ventral midline appears to occur at early stages in SBW development, however, the exact mechanism affecting cardiac or diaphragmatic development remains unclear. Similarly, mice harboring a targeted mutation in an amino acid (Arg709 to Cys) in the motor domain of NMHCII-B (*Myh10*) B^{R709C}/B^{R709C} exhibit a number of midline closure defects, including of both the thoracic and abdominal ventral midline, anterior (ventral) diaphragm, and the palate.[163] Yet, the cranial and infraumbilical VBW midline do develop fully. These mutants also display restricted cardiac atrioventricular cushion development resulting in a double outlet right ventricle. It is suggested that the *Myh10* gene defect results in reduced apoptosis, abnormal cell adhesion and ultimately failure of cells assembling at the midline.[163]

Murine models recapitulating FDH display some of the phenotypic elements of PC. In humans, loss of function mutations in porcupine (*PORCN*), an ER membrane O-acyl transferase results in FDH.[311] The key clinical features of skin hypoplasia, dental, and ocular anomalies, are seen in the null *Porcn* mutant.[118] This model displays, to a variable degree, exomphalos and sternal hypoplasia, but not other features of PC. *Porcn* is dedicated to Wnt palmitoylation and secretion demonstrating the critical role of Wnt signaling during body wall closure. Moreover, secondary thoracic and abdominal ventral midline development fails when Wnt is disrupted in the ventral mesoderm or ectoderm.[49,57,117]

TAS and LBWC are fatal embryonic syndromes where the ventral midline lacks any tissue cover, and the thoracic and/or abdominal organs are exposed in the amnion. They are generally associated with a wide array of congenital anomalies that include the limb, neural tube and craniofacial defects. Given their rarity and lethality no study to date has identified a specific genetic causation in humans. Yet, TAS can readily be observed in the *Tfap2α* null mouse, *Grhl2* mutant, and *Pitx2* null mice.[56–58,67,81] The expression of these genes in the ectoderm and LPM suggest their involvement in an essential epithelial-mesenchymal pathway, including regulation of canonical Wnt and Wnt-PCP signaling, that when lost prevents or halts SBW development at a very early stage[82,83] (also see Sections 4, 4.1, and 4.2.2). An interesting outstanding question raised by the *Tfap2α* and *Grhl2* models relates to the identity of the components of the proposed epithelial-mesenchymal signaling pathway.

Interestingly, a phenotypic spectrum representative of LBWC is present in various murine models of disturbed PCP protein function most likely linked to non-canonical Wnt signaling (Wnt-PCP). This is most pronounced in the $Vangl2^{Lp/+}$; $Scribble^{Crc/+}$double heterozygote, and $Ryk^{-/-}$; $Vangl2^{-/-}$double null but also presents with very low penetrance in $Scrib^{crc/crc}$, $Ror1^{-/-}$; $Ror2^{-/-}$ double homozygote, and $Ptk7^{chz/chz}$. The constellation of developmental anomalies displayed by these mutants include a ventral midline closure defect, neural tube closure defect, structural cardiac anomalies, anorectal malformation, and a variable degree of skeletal and hind limb deformities.[120,121,127,128,312] The pattern of congenital defects and the overall topographical appearance of these mutants is highly similar to reported miscarried human fetuses with severe forms of LBWC with the exception of the neural tube defect, exencephaly.[285,313] It is proposed that these various components of Wnt-PCP signaling contribute to collective tissue movements, including convergent extension, which impact on embryonic turning and posterior axis elongation, possibly at an early gastrulation phase and also during later cranial-caudal extension (see Section 3.7), leading to this unique pathology. A milder form of LBWC can be observed in the *Msx1-Msx2* double knockout and the *Msx2-Cre*; $Wls^{c/c}$ which prevents Wnt ligand secretion from the ectoderm. In both models, the secondary VBW fails to develop to a variable degree which is associated with fore- and hind limbs malformations.[77,116] As reported in human cases of LBWC, the VBW anomaly spares the thorax midline and is associated with bifid genitalia. However, the ventral organs in these murine models maintain a degree of mesenchymal-epithelial tissue cover as opposed to the complete schisis nature of the anomaly in humans. Moreover, *Msx1/2*, and *Msx2-cre*; *Wls* murine models are viable in late embryonic stages and fetal life, a rather unusual characteristic in human reports of LBWC.

One of the synonyms of LBWC is short umbilical cord syndrome, emphasizing that this constellation of defects is unique to the lower torso which again suggests an independent developmental mechanism such as disturbed mesenchymal cell migration restricted to the infraumbilical mesoderm (see Section 3.7).

6.2 | Ectopia cordis and sternal cleft

Ectopia cordis is a rare and lethal embryonic malformation usually encountered as a component in PC, or rarely as an isolated pathology. The exact mechanism leading to this unique defect is rather obscure, however it has been suggested that failure of cranial body folding or decreased growth of the thoracic VBW, leads to herniation of the heart outside the pericardial cavity. There is no animal model to date for pure ectopia cordis, and most of our knowledge on the pathology is derived from models of severe ventral midline closure defects or those mimicking PC.[49,74,100,117,163] Canonical Wnt signaling is essential for thoracic VBW closure and has been implicated in isolated ectopia cordis but this pathway is also essential for abdominal VBW closure.[49,117] The *Wls*$^{f/f}$; *Dermo1*$^{Cre/+}$ and *Lrp5/6*$^{f/f}$; *Dermo1*$^{Cre/+}$ mutants, which lack Wnt ligand expression (*Wls*$^{f/f}$; *Dermo1*$^{Cre/+}$) and intracellular canonical Wnt signaling (*Lrp5/6*$^{f/f}$; *Dermo1*$^{Cre/+}$) in the mesoderm, demonstrate failure of mesenchymal cell migration to the ventral midline from as early as E11.5.[49] In the absence of Wnt signaling, there is decreased cell survival and proliferation. The targets of Wnt signaling include the *Pitx2*-expressing and dermal cell populations (see Section 4.2.4). An additional question is whether myofibroblasts, a crucial cell population, also require Wnt signaling.

An isolated split sternum is not classified, at least clinically, under VBW closure defects. Nevertheless, there are many murine models displaying this defect, and they provide crucial mechanistic insight into sternum and thoracic VBW development and closure. A list of these models is provided in Table 2.

6.3 | Gastroschsisis

GS is the most commonly encountered VBW closure defect and carries the best clinical outcomes, yet its etiology is not at all well understood. Despite the mechanistic insight obtained from a handful of murine models of GS, it is essential to note that the generation of a true and representative animal model of the pathology is yet to be seen. The sporadic, isolated and low complexity nature of the pathology, coupled with defined environmental associations renders it difficult to predict target genetic or mechanistic pathways. Some genetic mouse models show features of VBW closure defects suggestive of GS, as discussed below.[121,133,134] The main debate regarding these models is that in human GS the eviscerated organs are free floating in the amniotic fluid. In murine models, the eviscerated organs sit in an exocoelomic space separated from the amnion, while the amnion maintains its attachment to the edges of the umbilical cord.[122] This unique configuration could be explained by the fact that following completion of turning in the murine embryo, the intra- and extraembryonic coeloms are continuous at the edges of the umbilical cord. Here, the PBW is deficient and a mesenchymal failure, restricted to a susceptible portion of the mesenchyme, could lead to gut herniation into the extraembryonic coelom rather into the amniotic cavity. Hence, the herniated gut contents are covered by the thin membranous visceral yolk sac and are not in direct contact with the amniotic fluid, contrary to what is seen in human GS. Despite this dilemma, these models of VBW closure defects are more in keeping phenotypically with GS rather than an exomphalos.

Mouse mutant models presenting a GS-like phenotype are scarce and can be observed mainly in the *Aclp*$^{-/-}$, *Bmp1*$^{-/-}$, *Barx1*$^{-/-}$, and to some extent in the *Hand1*$^{f/f}$:*Tlx2-Cre*, *Shroom*$^{-/-}$ and *Folbp* $^{-/-}$ mouse mutants.[61,69,133–135,147,168] *Bmp1* is expressed in the somatopleure of the VBW and in the mesoderm of the UR.[135] The *Bmp1* mouse mutant lacks the ventral mesoderm within the umbilicus that is normally continuous with the peritoneal mesoderm.[135] Similarly, selective deletion of *Hand1* within the PBW and LPM of the UR results in a GS phenotype.[69] These studies suggest that a cell population in the UR mesoderm is involved in the pathogenesis of GS. Furthermore, *Aclp* and *Bmp1* both regulate collagen structure.[135,314–316] ACLP increases the tensile strength of collagen fibrils while Bmp1 cleaves the C-terminus of collagen fibrils and also activates lysyl oxidase precursor that cross links collagen fibers.[135,314–316] In the amnion and VBW of E13.5 *Bmp1* mutants, the collagen fibers are defective and histologically resemble "barbed-wires" rather than straight fibrils.[135] Similarly, a small proportion of *Shroom*$^{-/-}$ mutants display a GS anomaly.[168] Shroom is an F-Actin binding protein and it is strongly expressed in the PBW from E9.5. *Shroom* mutants demonstrate defective actin sub-cellular localization and irregular cytoskeletal architecture. All these data indicate that mechanical changes within the UR tissue may be a contributory factor in the pathology of GS.

Mammalian models of GS have also been obtained by exposure to teratogens including carbon monoxide, cadmium and retinoic acid (reviewed by[317]). The

susceptibility to teratogens indicates there is a more sensitive tissue/domain within the developing VBW. The presence of a GS phenotype in the folate binding protein-1 (Folbp-1) model, and the partial recovery of the phenotype with folate supplementation further supports the presence of a susceptible region within the UR mesenchyme.[147] This would also explain the high prevalence of GS in pregnancies exposed to vasoactive recreational drugs. This vulnerability may be due to a structural weakness such as a thinner tissue, regions of higher ROS activity with different metabolic activity, and/or be due to tissue remodeling. Indeed, apoptosis is high within the UR and adjacent body wall mesenchyme[56] and there is also the regression of the right umbilical vein; this asymmetric regression has been proposed to make the right side weaker and be the reason why GS occurs predominantly on the right side.

While *Bmp1* and *Aclp* mutants provide insight into mechanisms of GS in the mouse, they do not phenotypically model *BMP1* and *AEPB1* (*ACLP*) autosomal recessive mutations in humans, which cause Ehlers-Danlos syndrome, classic-like 2 and osteogenesis imperfecta, type XIII, respectively. Neither syndrome is characterized by GS, although minor ventral wall anomalies (umbilical hernia, ventral hernia) have been reported in some patients with classic-like 2 Ehlers-Danlos syndrome.[318,319]

6.4 | Exomphalos

Exomphalos can be caused by defects at a number of stages of body wall closure e.g. failure in lateral body folding (Pitx2, Six5/6), delayed or stalled enclosure of the SBW (Tgfβ), failure of the umbilicus to close at E16.5 (Rock1/2). It is also possible that exomphalos results from a failure of gut rotation back into the abdominal cavity which physically obstructs VBW closure. Mutation in many genes have been shown to result in exomphalos (Table 2), a subset of which have been linked to exomphalos in humans (Table 3). The following discussion will focus on this latter group and highlight insights gained from these mouse models albeit with potential caveats.

Pitx2, is of interest, as it is a direct transcriptional target of canonical Wnt signaling and because heterozygous loss of function PITX2 mutations in humans results in Riegers-Axenfeld syndrome which can include VBW anomalies ranging from exomphalos to excessive umbilical skin.[228,267,320] While the *Pitx2*$^{-/-}$ mouse model can be used to understand mechanisms of PITX2 function in humans, there are, however, key differences. First, in humans the VBW anomaly is typically due to heterozygous loss of function mutations in *PITX2* whereas heterozygous *Pitx2*$^{+/-}$ mouse mutants are either normal or are characterized by a thinning of the VBW.[81,253] Thus, the homozygous *Pitx2*$^{-/-}$ mouse mutants which have a more extensive VBW closure phenotype encompassing both the thoracic and abdominal cavities, must be used for analysis.[80,81,85,253] Finally, in a subset of *Pitx2*$^{-/-}$ mouse mutants, body rotation is arrested which may contribute to the phenotype.[81,253] As the first step of embryo turning differs between mice and humans, mouse mutants with turning defects will not completely model the early steps of VBW development in humans. However, despite these differences, the *Pitx2*$^{-/-}$ mouse model can give insight into the mechanisms of VBW closure at later stages of development and how, the defect arises. Analysis of *Pitx2*$^{-/-}$ mutants has shown that there are defects in both the PBW and SBW (see Section 4.1; Tables 2 and S1). Reflecting the changes in the LPM and an intrinsic role of *Pitx2* in the hypaxial muscles, the musculature within the SBW is hypoplastic and disorganized.[82] A direct transcriptional target of Pitx2 in fetal musculature is procollagen lysyl hydroxylase 1 (Plod1) which may contribute to the phenotype.[321] Homozygous loss of PLOD1 in humans results in Ehlers-Danlos syndrome Kyphoscoliosis type IV, which has some overlapping features with Riegers-Axenfeld syndrome, including umbilical hernia.

6.5 | Bladder/CE

In animal models, bladder and CE is associated with decreased development of the infraumbilical mesenchyme (reviewed by Ludwig et al.[322]). In both disorders, the umbilicus is positioned more inferiorly. Additionally, the external genitalia, which arise from the LPM,[247] are often bifid. The bladder/CE may be due to insufficient mesenchyme to meet at the midline during the early lateral and caudal folding to form the PBW. Alternatively, the exstrophy may be due to insufficient merging of the mesenchyme along the midline at later stages of development due to decreased migration of mesenchymal cells from the umbilical area to the infraumbilical mesenchyme (see Section 3.7). Either deficit would render the VBW more prone to rupture or a failure to close.

Genetic profiling has identified many causative candidate genes (reviewed by[323,324]). The strongest candidate is ΔNTAF63, an anti-apoptotic factor, and one of the p63 isoforms. Decreased levels of ΔNTAF63 or changes in the p63 isoform ratios have been linked to bladder exstrophy in humans.[325,326] This bladder exstrophy phenotype is recapitulated in *p63* mouse mutants and analysis has focused on the alterations in bladder development.[78] The

midline defect is apparent by E11.5 indicative of an early change in PBW formation. ΔNTAF63 is expressed within the ventral bladder epithelium and the mouse mutants are characterized by increased cell death and decreased proliferation within the bladder epithelium. Additionally, the surrounding splanchnic mesoderm is hypoplastic which is linked to decreased expression of the *Fgf8* growth factor and *Msx1* transcription factor. Whether these alterations in bladder development are causative for the bladder exstrophy, is unclear. The bladder is an endodermal organ surrounded by splanchnic mesoderm and would not necessarily impact on the VBW, comprised of somatic lateral plate and paraxial mesoderm. P63 and its isoforms are also expressed in the epidermis where they control epithelial differentiation and epithelial-mesenchymal interactions (reviewed by Li et al.[327]). It is therefore possible that hypoplasia of the VBW is responsible for the bladder exstrophy in *p63* mouse mutants, or concurrent ΔNTAF63 function in both the bladder and VBW ectoderm is essential for VBW closure. Conditional knockout of ΔNTAF63 or p63 within different cell populations in mice will be required to resolve this question.

A putative model of bladder exstrophy can also be observed in the *Alx4* mouse mutant.[50,51] The infraumbilical ventral mesenchyme fails to develop resulting in hypoplastic lower VBW, anterior bladder wall and hypoplasia in the dorsal GT. In addition, this mutant demonstrates a SBW closure defect restricted to the abdominal region similar to that seen in an exomphalos major anomaly.[50,51] However, this model lacks the characteristic exteriorization (schisis) of the bladder or the associated epispadias anomaly, and the urethra shows complete anatomical development at E18.5. Nevertheless, mutations in the ALX4 gene have been identified as a potentially causative factor in human bladder exstrophy-epispadias complex.[210] One suggested mechanism, leading to this constellation of anomalies in the lower ventral midline, is ectopic Shh signaling within the caudal VBW. A dose-dependent increase in Shh signaling in the dorsal GT in the $Alx4^{Lst/+}$; $Gli3^{Xt/Xt}$; and $Alx4^{Lst/Lst}$; $Gli3^{Xt/Xt}$ double mutants also dictated the severity of dorsal GT hypoplasia. Nevertheless, the urethra demonstrated full anatomical development, excluding an epispadias component. These models similarly had the hypoplastic infraumbilical VBW, anterior bladder wall and the exomphalos type of anomaly that is seen in the $Alx4^{Lst/Lst}$ mutant.[50,51]

6.6 | Prune belly syndrome (PBS)

PBS is characterized in newborns/infants, predominantly male, by a thin and transparent ventral abdominal skin which has a "dried plum" appearance.[328] Hypoplasia of the abdominal straited musculature and of the smooth muscles around the bladder together with kidney anomalies are also common in PBS.[329] As these structures are derived from mesoderm[29] (reviewed in Reference 330), one hypothesis regarding its etiology highlights a defect of mesenchymal/mesodermal development.[329] Gene associations with PBS include mutation of the mesenchymal regulator HNF1β[331] as well as copy number variations in Bmp signaling components[332] known to drive muscle differentiation[333] and kidney morphogenesis[334] as well as urogenital development: urogenital defects are also a common feature of PBS.[329] Males with PBS can harbor mutations in X-linked FLNA, an actin binding protein that also engages with extracellular matrix receptors.[211] Mouse mutants for these candidate genes in humans, however, are either early embryonic lethal (*Hnf1β*[145]) or exhibit TAS (reduced dose of Bmps[93]) or exomphalos (*Bmp*[93] and *flna*[145]). *Bmp* mutants and the *Flna* mouse mutant *Dilp2* do, however, exhibit defects in mesodermal and mesenchymal growth[93,145] which may enable mechanistic insight into PBS. It will also be important to understand whether disruption to mesenchymal/mesodermal development leads to the type of ventral skin defects characteristic of PBS.

7 | FUTURE DIRECTIONS

An understanding of how the VBW develops gives insight into mechanisms of VBW anomalies which can arise due to failure in either PBW or SBW development. TAS, where all the thoracic and abdominal organs are exposed to the amnion, is the result of the failure of the PBW to form (e.g., Gata4, Furin) or the failure of invasion of SBW into the PBW (Tfap2α). Ectopia Cordis can arise due to a failure in the cranial fold or a defect in thoracic SBW closure while bladder and CE can be due to a failure in the caudal fold or in the anterior–posterior growth of lower abdominal VBW. Finally, exomphalos is due to an anomaly in the abdominal PBW or SBW or closure of the UR. While numerous mouse models have been generated that give molecular and cellular insight into mechanisms of VBW development, there are still significant gaps in our understanding. Particular challenges include that the genetic mouse models do not always recapitulate anomalies that occur in humans due to the same gene mutation. A fully representative model for GS in humans is still unavailable. In humans, VBW anomalies are often multifactorial making it difficult to pinpoint the genetic and environmental causes and although not yet clinically and genetically demonstrated may also arise by somatic mutations that result in mosaicism where the VBW consists of some cells carrying a gene mutation. As the VBW arises by large-scale tissue movements which involve collective cell movements, mosaic inactivation of gene

function may be particularly disruptive. Mosaic disruption in PCP genes that control large-scale tissue behaviors can be particularly impactful as demonstrated in the early thoracic wall and also, another tissue, the closing neural tube.[8,335]

Despite these reservations, an understanding of embryonic development will shed insight into mechanisms of VBW development and how anomalies may arise. Current gaps in our knowledge include:

1. The interplay between different cell populations during morphogenesis and cell differentiation within the VBW needs to be resolved. This includes an understanding of the role of Tgf-β signaling within the myofibroblasts which are proposed to be pioneering cells during VBW closure and of the PBW in promoting growth of the SBW. The potential role of coelomic cells, and physical contribution to VBW, also needs to be resolved.
2. A further understanding of cell movements, including large-scale tissue movements, during VBW closure is required. Growth of the body wall is predominantly ventral ward. However, studies in animal models have indicated considerable cell movements during VBW closure that contribute to growth along the other axes. These include convergent-extension movements at the leading edge of the thoracic body wall, extensive anterior–posterior movements of the thoracic LPM and mesenchymal migration inferiorly into the infraumbilical region.
3. Fate mapping studies indicate that the ectoderm and mesoderm move together in the thoracic SBW. The fate of the PBW mesoderm and ectoderm needs to be determined. Does the PBW undergo apoptosis or migration to contribute to other regions of the VBW.
4. Merging of epithelia: The epithelial behaviors during folding and merging in PBW development need to be analyzed. Do these merging processes create "weak points" that are vulnerable to rupture?
5. Analysis of p53/ROS activity/production, respectively, would identify cell populations that are particularly vulnerable to teratogens. If p53 or ROS activity is endogenously higher in a particular cell population, these cells would be expected to be more susceptible to teratogens which would increase p53/ROS activity above a particular threshold driving apoptosis.

ACKNOWLEDGMENTS

The authors work described in this review[8,71,99,100] was funded by The Wellcome Trust (095824/Z/11/Z), BBSRC (BB/G021074/1/BB and BB/W01730X/1), University of Manchester Constance Thornley Fellowship (105082), and British Heart Foundation (PG/14/1/30549). The authors thank Malcolm Logan and John Pizzey for critical reading of the review. PFW dedicates this review in memory of Francis Smith. The authors would also like to thank Michelle Francis and Evan Poole for help with generating Figures 1 and 2.

ORCID

Caroline Formstone https://orcid.org/0000-0002-5936-5149
Philippa Francis-West https://orcid.org/0000-0001-5179-5892

REFERENCES

1. Kaufman MH. *The Atlas of Mouse Development*. Elsevier Academic Press; 1994.
2. Gavrilov S, Lacy E. Genetic dissection of ventral folding morphogenesis in mouse: embryonic visceral endoderm-supplied BMP2 positions head and heart. *Curr Opin Genet Dev*. 2013; 23:461-469. doi:10.1016/j.gde.2013.04.001
3. Durland JL, Sferlazzo M, Logan M, Burke AC. Visualizing the lateral somitic frontier in the Prx1Cre transgenic mouse. *J Anat*. 2008;212:590-602. doi:10.1111/j.1469-7580.2008.00879.x
4. Kimura A, Inose H, Yano F, et al. Runx1 and Runx2 cooperate during sternal morphogenesis. *Development*. 2010;137: 1159-1167. doi:10.1242/dev.045005
5. Khabyuk J, Prols F, Draga M, Scaal M. Development of ribs and intercostal muscles in the chicken embryo. *J Anat*. 2022; 241:831-845. doi:10.1111/joa.13716
6. Beddington RS, Robertson EJ. Axis development and early asymmetry in mammals. *Cell*. 1999;96:195-209. doi:10.1016/s0092-8674(00)80560-7
7. Scaal M. Development of the amniote ventrolateral body wall. *Dev Dyn*. 2021;250:39-59. doi:10.1002/dvdy.193
8. Mao Y, Kuta A, Crespo-Enriquez I, et al. Dchs1-Fat4 regulation of polarized cell behaviours during skeletal morphogenesis. *Nat Commun*. 2016;7:11469. doi:10.1038/ncomms11469
9. Nichol PF, Corliss RF, Yamada S, Shiota K, Saijoh Y. Muscle patterning in mouse and human abdominal wall development and omphalocele specimens of humans. *Anat Rec*. 2012;295: 2129-2140. doi:10.1002/ar.22556
10. Deuchar EM, Parker FM. Further observations on axial rotation in rat embryos. *Acta Embryol Exp*. 1975;1:55-68.
11. Miller SA. Differential proliferation in morphogenesis of lateral body folds. *J Exp Zool*. 1982;221:205-211. doi:10.1002/jez.1402210211
12. Miller SA, White RD. Right-left asymmetry of cell proliferation predominates in mouse embryos undergoing clockwise axial rotation. *Anat Rec*. 1998;250:103-108. doi:10.1002/(SICI)1097-0185(199801)250:13.0.CO;2-S
13. Chevallier A. Role of the somitic mesoderm in the development of the rib cage of bird embryos. I. Origin of the sternal component and conditions for the development of the ribs. *J Embryol Exp Morphol*. 1975;33:291-311.
14. Christ B, Jacob HJ, Jacob M. Experimental studies on the development of the thoracic wall in chick embryos. *Experientia*. 1974;30:1449-1451. doi:10.1007/BF01919689

15. Nowicki JL, Takimoto R, Burke AC. The lateral somitic frontier: dorso-ventral aspects of anterio-posterior regionalization in avian embryos. *Mech Dev*. 2003;120:227-240. doi:10.1016/s0925-4773(02)00415-x
16. Olivera-Martinez I, Coltey M, Dhouailly D, Pourquie O. Mediolateral somitic origin of ribs and dermis determined by quail-chick chimeras. *Development*. 2000;127:4611-4617. doi:10.1242/dev.127.21.4611
17. Orioli D, Henkemeyer M, Lemke G, Klein R, Pawson T. Sek4 and Nuk receptors cooperate in guidance of commissural axons and in palate formation. *EMBO J*. 1996;15:6035-6049.
18. Sudo H, Takahashi Y, Tonegawa A, et al. Inductive signals from the somatopleure mediated by bone morphogenetic proteins are essential for the formation of the sternal component of avian ribs. *Dev Biol*. 2001;232:284-300. doi:10.1006/dbio.2001.0198
19. Bickley SR, Logan MP. Regulatory modulation of the T-box gene Tbx5 links development, evolution, and adaptation of the sternum. *Proc Natl Acad Sci U S A*. 2014;111:17917-17922. doi:10.1073/pnas.1409913111
20. Fell HB. The origin and developmental mechanics of the avian sternum. *Phil Trans R Soc London*. 1939;229:407-463.
21. Young M, Selleri L, Capellini TD. Genetics of scapula and pelvis development: an evolutionary perspective. *Curr Top Dev Biol*. 2019;132:311-349. doi:10.1016/bs.ctdb.2018.12.007
22. Dietrich S, Gruss P. Undulated phenotypes suggest a role of Pax-1 for the development of vertebral and extravertebral structures. *Dev Biol*. 1995;167:529-548. doi:10.1006/dbio.1995.1047
23. Henderson DJ, Conway SJ, Copp AJ. Rib truncations and fusions in the Sp2H mouse reveal a role for Pax3 in specification of the ventro-lateral and posterior parts of the somite. *Dev Biol*. 1999;209:143-158. doi:10.1006/dbio.1999.9215
24. Wallin J, Wilting J, Koseki H, Fritsch R, Christ B, Balling R. The role of Pax-1 in axial skeleton development. *Development*. 1994;120:1109-1121. doi:10.1242/dev.120.5.1109
25. Wood WM, Otis C, Etemad S, Goldhamer DJ. Development and patterning of rib primordia are dependent on associated musculature. *Dev Biol*. 2020;468:133-145. doi:10.1016/j.ydbio.2020.07.015
26. Chen JM. Studies on the morphogenesis of the mouse sternum. III. Experiments on the closure and segmentation of the sternal bands. *J Anat*. 1953;87:130-149.
27. Matsuoka T, Ahlberg PE, Kessaris N, et al. Neural crest origins of the neck and shoulder. *Nature*. 2005;436:347-355. doi:10.1038/nature03837
28. Mitchel K, Bergmann JM, Brent AE, et al. Hoxa5 activity across the lateral somitic frontier regulates development of the mouse sternum. *Front Cell Dev Biol*. 2022;10:806545. doi:10.3389/fcell.2022.806545
29. Christ B, Jacob M, Jacob HJ. On the origin and development of the ventrolateral abdominal muscles in the avian embryo. An experimental and ultrastructural study. *Anat Embryol*. 1983;166:87-101. doi:10.1007/BF00317946
30. Denetclaw WF Jr, Christ B, Ordahl CP. Location and growth of epaxial myotome precursor cells. *Development*. 1997;124:1601-1610. doi:10.1242/dev.124.8.1601
31. Bouzada J, Gemmell C, Konschake M, Tubbs RS, Pechriggl E, Sañudo J. New insights into the development of the anterior abdominal wall. *Front Surg*. 2022;9:863679. doi:10.3389/fsurg.2022.863679
32. Mekonen HK, Hikspoors JP, Mommen G, Eleonore KS, Lamers WH. Development of the epaxial muscles in the human embryo. *Clin Anat*. 2016;29:1031-1045. doi:10.1002/ca.22775
33. Naldaiz-Gastesi N, Bahri OA, Lopez de Munain A, McCullagh KJA, Izeta A. The panniculus carnosus muscle: an evolutionary enigma at the intersection of distinct research fields. *J Anat*. 2018;233:275-288. doi:10.1111/joa.12840
34. Fraser DA. The development of the skin of the back of the albino rat until the eruption of the first hairs. *Anat Rec*. 1928;38:203-223.
35. Munger GT, Munger BL. Differentiation of the anterior body wall and truncal epidermis and associated co-migration of cutaneous nerves and mesenchyme. *Anat Rec*. 1991;231:261-274. doi:10.1002/ar.1092310214
36. Panousopoulou E, Hobbs C, Mason I, Green JB, Formstone CJ. Epiboly generates the epidermal basal monolayer and spreads the nascent mammalian skin to enclose the embryonic body. *J Cell Sci*. 2016;129:1915-1927. doi:10.1242/jcs.180703
37. Holbrook KA. Structure and function of the developing human skin. *Physiology Biochemistry and Molecular Biology of the Skin*; 1983:64-101. Oxford University Press.
38. Candille SI, Raamsdonk CDV, Chen C, et al. Dorsoventral patterning of the mouse coat by Tbx15. *PLoS Biol*. 2004;2:E3. doi:10.1371/journal.pbio.0020003
39. Ohtola J, Myers J, Akhtar-Zaidi B, et al. Beta-catenin has sequential roles in the survival and specification of ventral dermis. *Development*. 2008;135:2321-2329. doi:10.1242/dev.021170
40. Chen D, Jarrell A, Guo C, Lang R, Atit R. Dermal beta-catenin activity in response to epidermal Wnt ligands is required for fibroblast proliferation and hair follicle initiation. *Development*. 2012;139:1522-1533. doi:10.1242/dev.076463
41. Tadeu AM, Horsley V. Notch signaling represses p63 expression in the developing surface ectoderm. *Development*. 2013;140:3777-3786. doi:10.1242/dev.093948
42. Nowicki JL, Burke AC. Hox genes and morphological identity: axial versus lateral patterning in the vertebrate mesoderm. *Development*. 2000;127:4265-4275. doi:10.1242/dev.127.19.4265
43. Burke AC, Nowicki JL. A new view of patterning domains in the vertebrate mesoderm. *Dev Cell*. 2003;4:159-165. doi:10.1016/s1534-5807(03)00033-9
44. Shimizu Y, Thumkeo D, Keel J, et al. ROCK-I regulates closure of the eyelids and ventral body wall by inducing assembly of actomyosin bundles. *J Cell Biol*. 2005;168:941-953. doi:10.1083/jcb.200411179
45. Snyder WH Jr, Chaffin L. An intermediate stage in the return of the intestines from the umbilical cord; embryo 37 mm. *Anat Rec*. 1952;113:451-457. doi:10.1002/ar.1091130407
46. Carapuco M, Novoa A, Bobola N, Mallo M. Hox genes specify vertebral types in the presomitic mesoderm. *Genes Dev*. 2005;19:2116-2121. doi:10.1101/gad.338705
47. Kaul A, Koster M, Neuhaus H, Braun T. Myf-5 revisited: loss of early myotome formation does not lead to a rib phenotype

in homozygous Myf-5 mutant mice. *Cell*. 2000;102:17-19. doi:10.1016/s0092-8674(00)00006-4
48. Tajbakhsh S, Rocancourt D, Cossu G, Buckingham M. Redefining the genetic hierarchies controlling skeletal myogenesis: Pax-3 and Myf-5 act upstream of MyoD. *Cell*. 1997;89:127-138. doi:10.1016/s0092-8674(00)80189-0
49. Snowball J, Ambalavanan M, Cornett B, Lang R, Whitsett J, Sinner D. Mesenchymal Wnt signaling promotes formation of sternum and thoracic body wall. *Dev Biol*. 2015;401:264-275. doi:10.1016/j.ydbio.2015.02.014
50. Matsumaru D, Haraguchi R, Moon AM, et al. Genetic analysis of the role of Alx4 in the coordination of lower body and external genitalia formation. *Eur J Hum Genet*. 2014;22:350-357. doi:10.1038/ejhg.2013.160
51. Qu S, Niswender KD, Ji Q, et al. Polydactyly and ectopic ZPA formation in Alx-4 mutant mice. *Development*. 1997;124:3999-4008. doi:10.1242/dev.124.20.3999
52. Hudson R, Taniguchi-Sidle A, Boras K, Wiggan O, Hamel PA. Alx-4, a transcriptional activator whose expression is restricted to sites of epithelial-mesenchymal interactions. *Dev Dyn*. 1998;213:159-169. doi:10.1002/(SICI)1097-0177(199810)213:23.0.CO;2-F
53. Qu S, Tucker SC, Zhao Q, deCrombrugghe B, Wisdom R. Physical and genetic interactions between Alx4 and Cart1. *Development*. 1999;126:359-369. doi:10.1242/dev.126.2.359
54. Iyyanar PPR, Wu Z, Lan Y, Hu YC, Jiang R. Alx1 deficient mice recapitulate craniofacial phenotype and reveal developmental basis of ALX1-related frontonasal dysplasia. *Front Cell Dev Biol*. 2022;10:777887. doi:10.3389/fcell.2022.777887
55. Zhao GQ, Eberspaecher H, Seldin MF, de Crombrugghe B. The gene for the homeodomain-containing protein Cart-1 is expressed in cells that have a chondrogenic potential during embryonic development. *Mech Dev*. 1994;48:245-254. doi:10.1016/0925-4773(94)90063-9
56. Brewer S, Williams T. Loss of AP-2alpha impacts multiple aspects of ventral body wall development and closure. *Dev Biol*. 2004;267:399-417. doi:10.1016/j.ydbio.2003.11.021
57. Zhang J, Hagopian-Donaldson S, Serbedzija G, et al. Neural tube, skeletal and body wall defects in mice lacking transcription factor AP-2. *Nature*. 1996;381:238-241. doi:10.1038/381238a0
58. Nottoli T, Hagopian-Donaldson S, Zhang J, Perkins A, Williams T. AP-2-null cells disrupt morphogenesis of the eye, face, and limbs in chimeric mice. *Proc Natl Acad Sci U S A*. 1998;95:13714-13719. doi:10.1073/pnas.95.23.13714
59. Schorle H, Meier P, Buchert M, Jaenisch R, Mitchell PJ. Transcription factor AP-2 essential for cranial closure and craniofacial development. *Nature*. 1996;381:235-238. doi:10.1038/381235a0
60. Lee Y, Fryer JD, Kang H, et al. ATXN1 protein family and CIC regulate extracellular matrix remodeling and lung alveolarization. *Dev Cell*. 2011;21:746-757. doi:10.1016/j.devcel.2011.08.017
61. Jayewickreme CD, Shivdasani RA. Control of stomach smooth muscle development and intestinal rotation by transcription factor BARX1. *Dev Biol*. 2015;405:21-32. doi:10.1016/j.ydbio.2015.05.024
62. Simon-Carrasco L et al. Inactivation of Capicua in adult mice causes T-cell lymphoblastic lymphoma. *Genes Dev*. 2017;31:1456-1468. doi:10.1101/gad.300244.117
63. Matsumaru D, Haraguchi R, Miyagawa S, et al. Genetic analysis of Hedgehog signaling in ventral body wall development and the onset of omphalocele formation. *PLoS One*. 2011;6:e16260. doi:10.1371/journal.pone.0016260
64. Mo R, Freer AM, Zinyk DL, et al. Specific and redundant functions of Gli2 and Gli3 zinc finger genes in skeletal patterning and development. *Development*. 1997;124:113-123. doi:10.1242/dev.124.1.113
65. Collier A, Liu A, Torkelson J, et al. Gibbin mesodermal regulation patterns epithelial development. *Nature*. 2022;606:188-196. doi:10.1038/s41586-022-04727-9
66. Li A, Hardy R, Stoner S, Tuckermann J, Seibel M, Zhou H. Deletion of mesenchymal glucocorticoid receptor attenuates embryonic lung development and abdominal wall closure. *PLoS One*. 2013;8:e63578. doi:10.1371/journal.pone.0063578
67. Pyrgaki C, Liu A, Niswander L. Grainyhead-like 2 regulates neural tube closure and adhesion molecule expression during neural fold fusion. *Dev Biol*. 2011;353:38-49. doi:10.1016/j.ydbio.2011.02.027
68. Nikolopoulou E, Hirst CS, Galea G, et al. Spinal neural tube closure depends on regulation of surface ectoderm identity and biomechanics by Grhl2. *Nat Commun*. 2019;10:2487. doi:10.1038/s41467-019-10164-6
69. Maska EL, Cserjesi P, Hua LL, Garstka ME, Brody HM, Morikawa Y. A Tlx2-Cre mouse line uncovers essential roles for hand1 in extraembryonic and lateral mesoderm. *Genesis*. 2010;48:479-484. doi:10.1002/dvg.20644
70. Grimm C, Sporle R, Schmid TE, et al. Isolation and embryonic expression of the novel mouse gene Hic1, the homologue of HIC1, a candidate gene for the Miller-Dieker syndrome. *Hum Mol Genet*. 1999;8:697-710. doi:10.1093/hmg/8.4.697
71. Pospichalova V, Tureckova J, Fafilek B, et al. Generation of two modified mouse alleles of the Hic1 tumor suppressor gene. *Genesis*. 2011;49:142-151. doi:10.1002/dvg.20719
72. Arostegui M, Scott RW, Bose K, Underhill TM. Cellular taxonomy of Hic1(+) mesenchymal progenitor derivatives in the limb: from embryo to adult. *Nat Commun*. 2022;13:4989. doi:10.1038/s41467-022-32695-1
73. Carter MG, Johns MA, Zeng X, et al. Mice deficient in the candidate tumor suppressor gene Hic1 exhibit developmental defects of structures affected in the Miller-Dieker syndrome. *Hum Mol Genet*. 2000;9:413-419. doi:10.1093/hmg/9.3.413
74. Manley NR, Barrow JR, Zhang T, Capecchi MR. Hoxb2 and hoxb4 act together to specify ventral body wall formation. *Dev Biol*. 2001;237:130-144. doi:10.1006/dbio.2001.0365
75. Barrow JR, Capecchi MR. Targeted disruption of the Hoxb-2 locus in mice interferes with expression of Hoxb-1 and Hoxb-4. *Development*. 1996;122:3817-3828. doi:10.1242/dev.122.12.3817
76. Ramirez-Solis R, Zheng H, Whiting J, Krumlauf R, Bradley A. Hoxb-4 (Hox-2.6) mutant mice show homeotic transformation of a cervical vertebra and defects in the closure of the sternal rudiments. *Cell*. 1993;73:279-294. doi:10.1016/0092-8674(93)90229-j
77. Ogi H, Suzuki K, Ogino Y, et al. Ventral abdominal wall dysmorphogenesis of Msx1/Msx2 double-mutant mice. *Anat Rec A Discov Mol Cell Evol Biol*. 2005;284:424-430. doi:10.1002/ar.a.20180

78. Cheng W, Jacobs WB, Zhang JJR, et al. DeltaNp63 plays an anti-apoptotic role in ventral bladder development. *Development*. 2006;133:4783-4792. doi:10.1242/dev.02621
79. Shih HP, Gross MK, Kioussi C. Expression pattern of the homeodomain transcription factor Pitx2 during muscle development. *Gene Expr Patterns*. 2007;7:441-451. doi:10.1016/j.modgep.2006.11.004
80. Kitamura K, Miura H, Miyagawa-Tomita S, et al. Mouse Pitx2 deficiency leads to anomalies of the ventral body wall, heart, extra- and periocular mesoderm and right pulmonary isomerism. *Development*. 1999;126:5749-5758. doi:10.1242/dev.126.24.5749
81. Lin CR, Kioussi C, O'Connell S, et al. Pitx2 regulates lung asymmetry, cardiac positioning and pituitary and tooth morphogenesis. *Nature*. 1999;401:279-282. doi:10.1038/45803
82. Eng D, Campbell A, Hilton T, Leid M, Gross MK, Kioussi C. Prediction of regulatory networks in mouse abdominal wall. *Gene*. 2010;469:1-8. doi:10.1016/j.gene.2010.08.008
83. Eng D, Ma HY, Xu J, Shih HP, Gross MK, Kiouss C. Loss of abdominal muscle in Pitx2 mutants associated with altered axial specification of lateral plate mesoderm. *PLoS One*. 2012;7:e42228. doi:10.1371/journal.pone.0042228
84. Hilton T, Gross MK, Kioussi C. Pitx2-dependent occupancy by histone deacetylases is associated with T-box gene regulation in mammalian abdominal tissue. *J Biol Chem*. 2010;285:11129-11142. doi:10.1074/jbc.M109.087429
85. Gage PJ, Suh H, Camper SA. Dosage requirement of Pitx2 for development of multiple organs. *Development*. 1999;126:4643-4651. doi:10.1242/dev.126.20.4643
86. Takahashi M, Tamura M, Sato S, Kawakami K. Mice doubly deficient in Six4 and Six5 show ventral body wall defects reproducing human omphalocele. *Dis Model Mech*. 2018;11. doi:10.1242/dmm.034611
87. Hargrave M, Wright E, Kun J, Emery J, Cooper L, Koopman P. Expression of the Sox11 gene in mouse embryos suggests roles in neuronal maturation and epithelio-mesenchymal induction. *Dev Dyn*. 1997;210:79-86. doi:10.1002/(SICI)1097-0177(199710)210:23.0.CO;2-6
88. Sock E, Rettig SD, Enderich J, Bösl MR, Tamm ER, Wegner M. Gene targeting reveals a widespread role for the high-mobility-group transcription factor Sox11 in tissue remodeling. *Mol Cell Biol*. 2004;24:6635-6644. doi:10.1128/MCB.24.15.6635-6644.2004
89. Bhattaram P, Penzo-Méndez A, Sock E, et al. Organogenesis relies on SoxC transcription factors for the survival of neural and mesenchymal progenitors. *Nat Commun*. 2010;1:9. doi:10.1038/ncomms1008
90. Purandare SM, Ware SM, Kwan KM, et al. A complex syndrome of left-right axis, central nervous system and axial skeleton defects in Zic3 mutant mice. *Development*. 2002;129:2293-2302. doi:10.1242/dev.129.9.2293
91. Klootwijk R, Franke B, van der Zee C, et al. A deletion encompassing Zic3 in bent tail, a mouse model for X-linked neural tube defects. *Hum Mol Genet*. 2000;9:1615-1622. doi:10.1093/hmg/9.11.1615
92. Goldman DC, Hackenmiller R, Nakayama T, et al. Mutation of an upstream cleavage site in the BMP4 prodomain leads to tissue-specific loss of activity. *Development*. 2006;133:1933-1942. doi:10.1242/dev.02368
93. Goldman DC, Donley N, Christian JL. Genetic interaction between Bmp2 and Bmp4 reveals shared functions during multiple aspects of mouse organogenesis. *Mech Dev*. 2009;126:117-127. doi:10.1016/j.mod.2008.11.008
94. Singh AP, Castranio T, Scott G, et al. Influences of reduced expression of maternal bone morphogenetic protein 2 on mouse embryonic development. *Sex Dev*. 2008;2:134-141. doi:10.1159/000143431
95. Sun J, Liu YH, Chen H, et al. Deficient Alk3-mediated BMP signaling causes prenatal omphalocele-like defect. *Biochem Biophys Res Commun*. 2007;360:238-243. doi:10.1016/j.bbrc.2007.06.049
96. Nerurkar NL, Mahadevan L, Tabin CJ. BMP signaling controls buckling forces to modulate looping morphogenesis of the gut. *Proc Natl Acad Sci U S A*. 2017;114:2277-2282. doi:10.1073/pnas.1700307114
97. Dünker N, Krieglstein K. Tgfbeta2 -/- Tgfbeta3 -/- double knockout mice display severe midline fusion defects and early embryonic lethality. *Anat Embryol*. 2002;206:73-83. doi:10.1007/s00429-002-0273-6
98. Matsunobu T, Torigoe K, Ishikawa M, et al. Critical roles of the TGF-beta type I receptor ALK5 in perichondrial formation and function, cartilage integrity, and osteoblast differentiation during growth plate development. *Dev Biol*. 2009;332:325-338. doi:10.1016/j.ydbio.2009.06.002
99. Aldeiri B, Roostalu U, Albertini A, Wong J, Morabito A, Cossu G. Transgelin-expressing myofibroblasts orchestrate ventral midline closure through TGFbeta signalling. *Development*. 2017;144:3336-3348. doi:10.1242/dev.152843
100. Aldeiri B, Roostalu U, Albertini A, et al. Abrogation of TGF-beta signalling in TAGLN expressing cells recapitulates pentalogy of Cantrell in the mouse. *Sci Rep*. 2018;8:3658. doi:10.1038/s41598-018-21948-z
101. Sanford LP, Ormsby I, Groot ACGD, et al. TGFbeta2 knockout mice have multiple developmental defects that are non-overlapping with other TGFbeta knockout phenotypes. *Development*. 1997;124:2659-2670. doi:10.1242/dev.124.13.2659
102. Dravis C, Henkemeyer M. Ephrin-B reverse signaling controls septation events at the embryonic midline through separate tyrosine phosphorylation-independent signaling avenues. *Dev Biol*. 2011;355:138-151. doi:10.1016/j.ydbio.2011.04.020
103. Davy A, Aubin J, Soriano P. Ephrin-B1 forward and reverse signaling are required during mouse development. *Genes Dev*. 2004;18:572-583. doi:10.1101/gad.1171704
104. Compagni A, Logan M, Klein R, Adams RH. Control of skeletal patterning by ephrinB1-EphB interactions. *Dev Cell*. 2003;5:217-230. doi:10.1016/s1534-5807(03)00198-9
105. Nichol PF, Corliss RF, Tyrrell JD, Graham B, Reeder A, Saijoh Y. Conditional mutation of fibroblast growth factor receptors 1 and 2 results in an omphalocele in mice associated with disruptions in ventral body wall muscle formation. *J Pediatr Surg*. 2011;46:90-96. doi:10.1016/j.jpedsurg.2010.09.066
106. Boylan M, Anderson MJ, Ornitz DM, Lewandoski M. The Fgf8 subfamily (Fgf8, Fgf17 and Fgf18) is required for closure of the embryonic ventral body wall. *Development*. 2020;147. doi:10.1242/dev.189506
107. Roebroek AJ, Umans L, Pauli IG, et al. Failure of ventral closure and axial rotation in embryos lacking the proprotein

convertase Furin. *Development*. 1998;125:4863-4876. doi:10.1242/dev.125.24.4863
108. Eggenschwiler J, Ludwig T, Fisher P, Leighton PA, Tilghman SM, Efstratiadis A. Mouse mutant embryos overexpressing IGF-II exhibit phenotypic features of the Beckwith-Wiedemann and Simpson-Golabi-Behmel syndromes. *Genes Dev*. 1997;11:3128-3142. doi:10.1101/gad.11.23.3128
109. Orr-Urtreger A, Bedford MT, Do MS, Eisenbach L, Lonai P. Developmental expression of the alpha receptor for platelet-derived growth factor, which is deleted in the embryonic lethal Patch mutation. *Development*. 1992;115:289-303. doi:10.1242/dev.115.1.289
110. Orr-Urtreger A, Lonai P. Platelet-derived growth factor-A and its receptor are expressed in separate, but adjacent cell layers of the mouse embryo. *Development*. 1992;115:1045-1058. doi:10.1242/dev.115.4.1045
111. Schatteman GC, Morrison-Graham K, van Koppen A, Weston JA, Bowen-Pope DF. Regulation and role of PDGF receptor alpha-subunit expression during embryogenesis. *Development*. 1992;115:123-131. doi:10.1242/dev.115.1.123
112. Soriano P. The PDGF alpha receptor is required for neural crest cell development and for normal patterning of the somites. *Development*. 1997;124:2691-2700. doi:10.1242/dev.124.14.2691
113. Qian C, Wong CWY, Wu Z, et al. Stage specific requirement of platelet-derived growth factor receptor-alpha in embryonic development. *PLoS One*. 2017;12:e0184473. doi:10.1371/journal.pone.0184473
114. Payne J, Shibasaki F, Mercola M. Spina bifida occulta in homozygous Patch mouse embryos. *Dev Dyn*. 1997;209:105-116. doi:10.1002/(SICI)1097-0177(199705)209:13.0.CO;2-0
115. Klinghoffer RA, Hamilton TG, Hoch R, Soriano P. An allelic series at the PDGFalphaR locus indicates unequal contributions of distinct signaling pathways during development. *Dev Cell*. 2002;2:103-113. doi:10.1016/s1534-5807(01)00103-4
116. Zhang L, Li H, Yu J, et al. Ectodermal Wnt signaling regulates abdominal myogenesis during ventral body wall development. *Dev Biol*. 2014;387:64-72. doi:10.1016/j.ydbio.2013.12.027
117. Joeng KS, Schumacher CA, Zylstra-Diegel CR, Long F, Williams BO. Lrp5 and Lrp6 redundantly control skeletal development in the mouse embryo. *Dev Biol*. 2011;359:222-229. doi:10.1016/j.ydbio.2011.08.020
118. Barrott JJ, Cash GM, Smith AP, Barrow JR, Murtaugh LC. Deletion of mouse Porcn blocks Wnt ligand secretion and reveals an ectodermal etiology of human focal dermal hypoplasia/Goltz syndrome. *Proc Natl Acad Sci U S A*. 2011;108:12752-12757. doi:10.1073/pnas.1006437108
119. Devenport D, Fuchs E. Planar polarization in embryonic epidermis orchestrates global asymmetric morphogenesis of hair follicles. *Nat Cell Biol*. 2008;10:1257-1268. doi:10.1038/ncb1784
120. Murdoch JN, Damrau C, Paudyal A, et al. Genetic interactions between planar cell polarity genes cause diverse neural tube defects in mice. *Dis Model Mech*. 2014;7:1153-1163. doi:10.1242/dmm.016758
121. Murdoch JN, Henderson DJ, Doudney K, et al. Disruption of scribble (Scrb1) causes severe neural tube defects in the circletail mouse. *Hum Mol Genet*. 2003;12:87-98. doi:10.1093/hmg/ddg014
122. Carnaghan H, Roberts T, Savery D, et al. Novel exomphalos genetic mouse model: the importance of accurate phenotypic classification. *J Pediatr Surg*. 2013;48:2036-2042. doi:10.1016/j.jpedsurg.2013.04.010
123. Murdoch JN, Rachel RA, Shah S, et al. Circletail, a new mouse mutant with severe neural tube defects: chromosomal localization and interaction with the loop-tail mutation. *Genomics*. 2001;78:55-63. doi:10.1006/geno.2001.6638
124. Pearson HB, Perez-Mancera PA, Dow LE, et al. SCRIB expression is deregulated in human prostate cancer, and its deficiency in mice promotes prostate neoplasia. *J Clin Invest*. 2011;121:4257-4267. doi:10.1172/JCI58509
125. Lu X, Borchers AGM, Jolicoeur C, Rayburn H, Baker JC, Tessier-Lavigne M. PTK7/CCK-4 is a novel regulator of planar cell polarity in vertebrates. *Nature*. 2004;430:93-98. doi:10.1038/nature02677
126. Paudyal A, Damrau C, Patterson VL, et al. The novel mouse mutant, chuzhoi, has disruption of Ptk7 protein and exhibits defects in neural tube, heart and lung development and abnormal planar cell polarity in the ear. *BMC Dev Biol*. 2010;10:87. doi:10.1186/1471-213X-10-87
127. Andre P, Wang Q, Wang N, et al. The Wnt coreceptor Ryk regulates Wnt/planar cell polarity by modulating the degradation of the core planar cell polarity component Vangl2. *J Biol Chem*. 2012;287:44518-44525. doi:10.1074/jbc.M112.414441
128. Ho HY, Susman MW, Bikoff JB, et al. Wnt5a-Ror-Dishevelled signaling constitutes a core developmental pathway that controls tissue morphogenesis. *Proc Natl Acad Sci U S A*. 2012;109:4044-4051. doi:10.1073/pnas.1200421109
129. Nomi M, Oishi I, Kani S, et al. Loss of mRor1 enhances the heart and skeletal abnormalities in mRor2-deficient mice: redundant and pleiotropic functions of mRor1 and mRor2 receptor tyrosine kinases. *Mol Cell Biol*. 2001;21:8329-8335. doi:10.1128/MCB.21.24.8329-8335.2001
130. Yamaguchi TP, Bradley A, McMahon AP, Jones S. A Wnt5a pathway underlies outgrowth of multiple structures in the vertebrate embryo. *Development*. 1999;126:1211-1223. doi:10.1242/dev.126.6.1211
131. Doyonnas R, Kershaw DB, Duhme C, et al. Anuria, omphalocele, and perinatal lethality in mice lacking the CD34-related protein podocalyxin. *J Exp Med*. 2001;194:13-27. doi:10.1084/jem.194.1.13
132. Abdelhamed ZA, Natarajan S, Wheway G, et al. The Meckel-Gruber syndrome protein TMEM67 controls basal body positioning and epithelial branching morphogenesis in mice via the non-canonical Wnt pathway. *Dis Model Mech*. 2015;8:527-541. doi:10.1242/dmm.019083
133. Danzer E, Layne MD, Auber F, et al. Gastroschisis in mice lacking aortic carboxypeptidase-like protein is associated with a defect in neuromuscular development of the eviscerated intestine. *Pediatr Res*. 2010;68:23-28. doi:10.1203/PDR.0b013e3181e17c75
134. Layne MD, Yet SF, Maemura K, et al. Impaired abdominal wall development and deficient wound healing in mice lacking aortic carboxypeptidase-like protein. *Mol Cell Biol*. 2001;21:5256-5261. doi:10.1128/MCB.21.15.5256-5261.2001
135. Suzuki N, Labosky PA, Furuta Y, et al. Failure of ventral body wall closure in mouse embryos lacking a procollagen

C-proteinase encoded by Bmp1, a mammalian gene related to Drosophila tolloid. *Development*. 1996;122:3587-3595. doi:10.1242/dev.122.11.3587

136. Zhu X, Huang S, Zhang L, et al. Constitutive activation of ectodermal beta-catenin induces ectopic outgrowths at various positions in mouse embryo and affects abdominal ventral body wall closure. *PLoS One*. 2014;9:e92092. doi:10.1371/journal.pone.0092092
137. Coppolino MG, Woodside MJ, Demaurex N, Grinstein S, St-Arnaud R, Dedhar S. Calreticulin is essential for integrin-mediated calcium signalling and cell adhesion. *Nature*. 1997;386:843-847. doi:10.1038/386843a0
138. De Almeida I, Oliveira NMM, Randall RA, et al. Calreticulin is a secreted BMP antagonist, expressed in Hensen's node during neural induction. *Dev Biol*. 2017;421:161-170. doi:10.1016/j.ydbio.2016.12.001
139. Groenendyk J, Michalak M. Disrupted WNT signaling in mouse embryonic stem cells in the absence of calreticulin. *Stem Cell Rev Rep*. 2014;10:191-206. doi:10.1007/s12015-013-9488-6
140. Rauch F, Prud'homme J, Arabian A, Dedhar S, St-Arnaud R. Heart, brain, and body wall defects in mice lacking calreticulin. *Exp Cell Res*. 2000;256:105-111. doi:10.1006/excr.2000.4818
141. Bartolini B, Thelin MA, Svensson L, et al. Iduronic acid in chondroitin/dermatan sulfate affects directional migration of aortic smooth muscle cells. *PLoS One*. 2013;8:e66704. doi:10.1371/journal.pone.0066704
142. Radek KA, Taylor KR, Gallo RL. FGF-10 and specific structural elements of dermatan sulfate size and sulfation promote maximal keratinocyte migration and cellular proliferation. *Wound Repair Regen*. 2009;17:118-126. doi:10.1111/j.1524-475X.2008.00449.x
143. Gustafsson R, Stachtea X, Maccarana M, et al. Dermatan sulfate epimerase 1 deficient mice as a model for human abdominal wall defects. *Birth Defects Res A Clin Mol Teratol*. 2014;100:712-720. doi:10.1002/bdra.23300
144. Maccarana M, Kalamajski S, Kongsgaard M, Magnusson SP, Oldberg Å, Malmström A. Dermatan sulfate epimerase 1-deficient mice have reduced content and changed distribution of iduronic acids in dermatan sulfate and an altered collagen structure in skin. *Mol Cell Biol*. 2009;29:5517-5528. doi:10.1128/MCB.00430-09
145. Lian G, Kanaujia S, Wong T, Sheen V. FilaminA and Formin2 regulate skeletal, muscular, and intestinal formation through mesenchymal progenitor proliferation. *PLoS One*. 2017;12:e0189285. doi:10.1371/journal.pone.0189285
146. Hart AW, Morgan JE, Schneider J, et al. Cardiac malformations and midline skeletal defects in mice lacking filamin A. *Hum Mol Genet*. 2006;15:2457-2467. doi:10.1093/hmg/ddl168
147. Spiegelstein O, Mitchell LE, Merriweather MY, et al. Embryonic development of folate binding protein-1 (Folbp1) knockout mice: effects of the chemical form, dose, and timing of maternal folate supplementation. *Dev Dyn*. 2004;231:221-231. doi:10.1002/dvdy.20107
148. Komada M, Soriano P. Hrs, a FYVE finger protein localized to early endosomes, is implicated in vesicular traffic and required for ventral folding morphogenesis. *Genes Dev*. 1999;13:1475-1485. doi:10.1101/gad.13.11.1475
149. Follit JA, San Agustin JT, Xu F, et al. The Golgin GMAP210/-TRIP11 anchors IFT20 to the Golgi complex. *PLoS Genet*. 2008;4:e1000315. doi:10.1371/journal.pgen.1000315
150. Smits P, Bolton AD, Funari V, et al. Lethal skeletal dysplasia in mice and humans lacking the golgin GMAP-210. *N Engl J Med*. 2010;362:206-216. doi:10.1056/NEJMoa0900158
151. Yamada R, Mizutani-Koseki Y, Koseki H, Takahashi N. Requirement for Mab21l2 during development of murine retina and ventral body wall. *Dev Biol*. 2004;274:295-307. doi:10.1016/j.ydbio.2004.07.016
152. Baldessari D, Badaloni A, Longhi R, Zappavigna V, Consalez GG. MAB21L2, a vertebrate member of the male-abnormal 21 family, modulates BMP signaling and interacts with SMAD1. *BMC Cell Biol*. 2004;5:48. doi:10.1186/1471-2121-5-48
153. Stumpo DJ, Bock CB, Tuttle JS, Blackshear PJ. MARCKS deficiency in mice leads to abnormal brain development and perinatal death. *Proc Natl Acad Sci U S A*. 1995;92:944-948. doi:10.1073/pnas.92.4.944
154. Boucherat O, Nadeau V, Berube-Simard FA, Charron J, Jeannotte L. Crucial requirement of ERK/MAPK signaling in respiratory tract development. *Development*. 2014;141:3197-3211. doi:10.1242/dev.110254
155. Abell AN, Rivera-Perez JA, Cuevas BD, et al. Ablation of MEKK4 kinase activity causes neurulation and skeletal patterning defects in the mouse embryo. *Mol Cell Biol*. 2005;25:8948-8959. doi:10.1128/MCB.25.20.8948-8959.2005
156. Chi H, Sarkisian MR, Rakic P, Flavell RA. Loss of mitogen-activated protein kinase kinase kinase 4 (MEKK4) results in enhanced apoptosis and defective neural tube development. *Proc Natl Acad Sci U S A*. 2005;102:3846-3851. doi:10.1073/pnas.0500026102
157. Zhang P, Liégeois NJ, Wong C, et al. Altered cell differentiation and proliferation in mice lacking p57KIP2 indicates a role in Beckwith-Wiedemann syndrome. *Nature*. 1997;387:151-158. doi:10.1038/387151a0
158. Hartmann D, De Strooper B, Saftig P. Presenilin-1 deficiency leads to loss of Cajal-Retzius neurons and cortical dysplasia similar to human type 2 lissencephaly. *Curr Biol*. 1999;9:719-727. doi:10.1016/s0960-9822(99)80331-5
159. Hoelzl MA, Heby-Henricson K, Gerling M, et al. Differential requirement of SUFU in tissue development discovered in a hypomorphic mouse model. *Dev Biol*. 2017;429:132-146. doi:10.1016/j.ydbio.2017.06.037
160. Guo H, Huang R, Semba S, et al. Ablation of smooth muscle caldesmon affects the relaxation kinetics of arterial muscle. *Pflugers Arch*. 2013;465:283-294. doi:10.1007/s00424-012-1178-8
161. Putz S et al. Caldesmon ablation in mice causes umbilical herniation and alters contractility of fetal urinary bladder smooth muscle. *J Gen Physiol*. 2021;153. doi:10.1085/jgp.202012776
162. Ma X, Adelstein RS. The role of vertebrate nonmuscle myosin II in development and human disease. *Bioarchitecture*. 2014b;4:88-102. doi:10.4161/bioa.29766
163. Ma X, Adelstein RS. A point mutation in Myh10 causes major defects in heart development and body wall closure. *Circ Cardiovasc Genet*. 2014a;7:257-265. doi:10.1161/CIRCGENETICS.113.000455

164. Tullio AN, Accili D, Ferrans VJ, et al. Nonmuscle myosin II-B is required for normal development of the mouse heart. *Proc Natl Acad Sci U S A*. 1997;94:12407-12412. doi:10.1073/pnas.94.23.12407
165. Thumkeo D, Shimizu Y, Sakamoto S, Yamada S, Narumiya S. ROCK-I and ROCK-II cooperatively regulate closure of eyelid and ventral body wall in mouse embryo. *Genes Cells*. 2005;10:825-834. doi:10.1111/j.1365-2443.2005.00882.x
166. Shi J, Wei L. Rho kinases in embryonic development and stem cell research. *Arch Immunol Ther Exp (Warsz)*. 2022;70:4. doi:10.1007/s00005-022-00642-z
167. Goering JP, Wenger LW, Stetsiv M, et al. In-frame deletion of SPECC1L microtubule association domain results in gain-of-function phenotypes affecting embryonic tissue movement and fusion events. *Hum Mol Genet*. 2021;31:18-31. doi:10.1093/hmg/ddab211
168. Hildebrand JD, Soriano P. Shroom, a PDZ domain-containing actin-binding protein, is required for neural tube morphogenesis in mice. *Cell*. 1999;99:485-497. doi:10.1016/s0092-8674(00)81537-8
169. van de Vis RAJ, Moustakas A, van der Heide LP. NUAK1 and NUAK2 fine-tune TGF-beta signaling. *Cancers*. 2021;13. doi:10.3390/cancers13133377
170. Hirano M, Kiyonari H, Inoue A, et al. A new serine/threonine protein kinase, Omphk1, essential to ventral body wall formation. *Dev Dyn*. 2006;235:2229-2237. doi:10.1002/dvdy.20823
171. Ohmura T, Shioi G, Hirano M, Aizawa S. Neural tube defects by NUAK1 and NUAK2 double mutation. *Dev Dyn*. 2012;241:1350-1364. doi:10.1002/dvdy.23816
172. Kakizaki T, Oriuchi N, Yanagawa Y. GAD65/GAD67 double knockout mice exhibit intermediate severity in both cleft palate and omphalocele compared with GAD67 knockout and VGAT knockout mice. *Neuroscience*. 2015;288:86-93. doi:10.1016/j.neuroscience.2014.12.030
173. Oh WJ, Westmoreland JJ, Summers R, Condie BG. Cleft palate is caused by CNS dysfunction in Gad1 and Viaat knockout mice. *PLoS One*. 2010;5:e9758. doi:10.1371/journal.pone.0009758
174. Saito K, Kakizaki T, Hayashi R, et al. The physiological roles of vesicular GABA transporter during embryonic development: a study using knockout mice. *Mol Brain*. 2010;3:40. doi:10.1186/1756-6606-3-40
175. Sibgatullina G, Al Ebrahim R, Gilizhdinova K, Tokmakova A, Malomouzh A. Differentiation of myoblasts in culture: focus on serum and GABA. *Cells Tissues Organs*. 2023;213:203-212. doi:10.1159/000529839
176. Nilius B. Chloride channels go cell cycling. *J Physiol*. 2001;532:581. doi:10.1111/j.1469-7793.2001.0581e.x
177. Wojcik SM, Katsurabayashi S, Guillemin I, et al. A shared vesicular carrier allows synaptic corelease of GABA and glycine. *Neuron*. 2006;50:575-587. doi:10.1016/j.neuron.2006.04.016
178. Hubner CA, Stein V, Hermans-Borgmeyer I, et al. Disruption of KCC2 reveals an essential role of K-Cl cotransport already in early synaptic inhibition. *Neuron*. 2001;30:515-524. doi:10.1016/s0896-6273(01)00297-5
179. Grote P, Wittler L, Hendrix D, et al. The tissue-specific lncRNA Fendrr is an essential regulator of heart and body wall development in the mouse. *Dev Cell*. 2013;24(2):206-214. doi:10.1016/j.devcel.2012.12.012
180. Hu Y, Baud V, Delhase M, et al. Abnormal morphogenesis but intact IKK activation in mice lacking the IKKalpha subunit of IkappaB kinase. *Science*. 1999;284(5412):316-320. doi:10.1126/science.284.5412.316
181. Szumska D, Pieles G, Essalmani R, et al. VACTERL/caudal regression/Currarino syndrome-like malformations in mice with mutation in the proprotein convertase Pcsk5. *Genes Dev*. 2008;22(11):1465-1477. doi:10.1101/gad.479408
182. Yadav SP, Sharma NK, Liu C, Dong L, Li T, Swaroop A. Centrosomal protein CP110 controls maturation of the mother centriole during cilia biogenesis. *Development*. 2016;143(9):1491-1501. doi:10.1242/dev.130120
183. Keady BT, Samtani R, Tobita K, et al. IFT25 links the signal-dependent movement of Hedgehog components to intraflagellar transport. *Dev Cell*. 2012;22(5):940-951. doi:10.1016/j.devcel.2012.04.009
184. Hsu CY, Chang NC, Lee MW, et al. LUZP deficiency affects neural tube closure during brain development. *Biochem Biophys Res Commun*. 2008;376(3):466-471. doi:10.1016/j.bbrc.2008.08.170
185. Radhakrishna U, Nath SK, McElreavey K, et al. Genome-wide linkage and copy number variation analysis reveals 710 kb duplication on chromosome 1p31.3 responsible for autosomal dominant omphalocele. *J Med Genet*. 2012;49(4):270-276.
186. Chen CP, Lin CJ, Chen YY, et al. 3q26.31-q29 duplication and 9q34.3 microdeletion associated with omphalocele, ventricular septal defect, abnormal first-trimester maternal serum screening and increased nuchal translucency: prenatal diagnosis and aCGH characterization. *Gene*. 2013;532(1):80-86. doi:10.1016/j.gene.2013.09.025
187. Wilson GN, Dasouki M, Barr M. Further delineation of the dup(3q) syndrome. *Am J Med Genet*. 1985;22(1):117-123. doi:10.1002/ajmg.1320220113
188. Ounap K, Ilus T, Bartsch O. A girl with inverted triplication of chromosome 3q25.3 —> q29 and multiple congenital anomalies consistent with 3q duplication syndrome. *Am J Med Genet A*. 2005;134(4):434-438. doi:10.1002/ajmg.a.30134
189. Caspary T, Cleary MA, Perlman EJ, Zhang P, Elledge SJ, Tilghman SM. Oppositely imprinted genes p57(Kip2) and igf2 interact in a mouse model for Beckwith-Wiedemann syndrome. *Genes Dev*. 1999;13(23):3115-3124. doi:10.1101/gad.13.23.3115
190. Watanabe H, Yamanaka T. A possible relationship between Beckwith-Wiedemann syndrome, urinary tract anomaly and prune belly syndrome. *Clin Genet*. 1990;38(6):410-414. doi:10.1111/j.1399-0004.1990.tb03605.x
191. Lam WW, Hatada I, Ohishi S, et al. Analysis of germline CDKN1C (p57KIP2) mutations in familial and sporadic Beckwith-Wiedemann syndrome (BWS) provides a novel genotype-phenotype correlation. *J Med Genet*. 1999;36(7):518-523.
192. Engel JR, Smallwood A, Harper A, et al. Epigenotype-phenotype correlations in Beckwith-Wiedemann syndrome. *J Med Genet*. 2000;37(12):921-926. doi:10.1136/jmg.37.12.921
193. Sinico M, Touboul C, Haddad B, et al. Giant omphalocele and "prune belly" sequence as components of the Beckwith-Wiedemann syndrome. *Am J Med Genet A*. 2004;129A(2):198-200. doi:10.1002/ajmg.a.30129
194. Feldkamp ML, Botto LD, Amar E, et al. Cloacal exstrophy: an epidemiologic study from the international clearinghouse for

birth defects surveillance and research. *Am J Med Genet C Semin Med Genet*. 2011;157C:333-343. doi:10.1002/ajmg.c.30317
195. Aziz MA. Anatomical defects in a case of trisomy 13 with a D/D translocation. *Teratology*. 1980;22(2):217-227. doi:10.1002/tera.1420220211
196. Nyberg DA, Fitzsimmons J, Mack LA, et al. Chromosomal abnormalities in fetuses with omphalocele. Significance of omphalocele contents. *J Ultrasound Med*. 1989;8(6):299-308. doi:10.7863/jum.1989.8.6.299
197. De Veciana M, Major CA, Porto M. Prediction of an abnormal karyotype in fetuses with omphalocele. *Prenat Diagn*. 1994;14(6):487-492. doi:10.1002/pd.1970140613
198. Chitayat D, Toi A, Babul R, et al. Omphalocele in Miller-Dieker syndrome: expanding the phenotype. *Am J Med Genet*. 1997;69(3):293-298.
199. Moore CA, Harmon JP, Padilla LM, Castro VB, Weaver DD. Neural tube defects and omphalocele in trisomy 18. *Clin Genet*. 1988;34(2):98-103. doi:10.1111/j.1399-0004.1988.tb02843.x
200. McInerney-Leo AM, Harris JE, Gattas M, et al. Fryns syndrome associated with recessive mutations in PIGN in two separate families. *Hum Mutat*. 2016;37(7):695-702. doi:10.1002/humu.22994
201. Sun L, Yang X, Xu Y, Sun S, Wu Q. Prenatal diagnosis of familial recessive PIGN mutation associated with multiple anomalies: a case report. *Taiwan J Obstet Gynecol*. 2021;60(3):530-533. doi:10.1016/j.tjog.2021.03.026
202. Longoni L, D'Apolito V, Cianci P, Selicorni A. Omphalocele in a patient with Noonan syndrome. *Clin Dysmorphol*. 2012;21(4):215-217. doi:10.1097/MCD.0b013e3283590a5a
203. Serra G, Felice S, Antona V, et al. Cardio-facio-cutaneous syndrome and gastrointestinal defects: report on a newborn with 19p13.3 deletion including the MAP 2 K2 gene. *Ital J Pediatr*. 2022;48(1):65. doi:10.1186/s13052-022-01241-6
204. Chen CP. Chromosomal abnormalities associated with omphalocele. *Taiwan J Obstet Gynecol*. 2007;46(1):1-8. doi:10.1016/S1028-4559(08)60099-6
205. Torfs CP, Honoré LH, Curry CJ. Is there an association of Down syndrome and omphalocele? *Am J Med Genet*. 1997;73(4):400-403.
206. Bedei I, Gloning KP, Joyeux L, et al. Turner syndrome-omphalocele association: incidence, karyotype, phenotype and fetal outcome. *Prenat Diagn*. 2023;43(2):183-191. doi:10.1002/pd.6302
207. Goldstein I, Drugan A. Cystic hygroma and omphalocele at 11 weeks in a fetus with monosomy X. *Prenat Diagn*. 2006;26(4):381-382. doi:10.1002/pd.1409
208. Samejima N, Ito S, Nakajima S, Ikeda K. Omphalocele and focal dermal hypoplasia. *Z Kinderchir*. 1981;34(3):284-289. doi:10.1055/s-2008-1063361
209. Alkindi S, Battin M, Aftimos S, Purvis D. Focal dermal hypoplasia due to a novel mutation in a boy with Klinefelter syndrome. *Pediatr Dermatol*. 2013;30(4):476-479. doi:10.1111/pde.12031
210. Chen CH, Bournat JC, Wilken N, et al. Variants in ALX4 and their association with genitourinary defects. *Andrology*. 2020;8:1243-1255. doi:10.1111/andr.12815
211. Iqbal NS, Jascur TA, Harrison SM, et al. Prune belly syndrome in surviving males can be caused by hemizygous missense mutations in the X-linked Filamin A gene. *BMC Med Genet*. 2020;21:38. doi:10.1186/s12881-020-0973-x
212. Robertson SP, Twigg SR, Sutherland-Smith AJ, et al. Localized mutations in the gene encoding the cytoskeletal protein filamin A cause diverse malformations in humans. *Nat Genet*. 2003;33(4):487-491. doi:10.1038/ng1119
213. Sankararaman S, Kurepa D, Shen Y, Kakkilaya V, Ursin S, Chen H. Otopalatodigital syndrome type 2 in a male infant: a case report with a novel sequence variation. *J Pediatr Genet*. 2013;2(1):33-36. doi:10.3233/PGE-13045
214. Naudion S, Moutton S, Coupry I, et al. Fetal phenotypes in otopalatodigital spectrum disorders. *Clin Genet*. 2016;89(3):371-377. doi:10.1111/cge.12679
215. Luo X, Yang Z, Zeng J, et al. Mutation of FLNA attenuating the migration of abdominal muscles contributed to Melnick-Needles syndrome (MNS) in a family with recurrent miscarriage. *Mol Genet Genomic Med*. 2023;11(5):e2145. doi:10.1002/mgg3.2145
216. Li C, Marles SL, Greenberg CR, et al. Manitoba Oculotrichoanal (MOTA) syndrome: report of eight new cases. *Am J Med Genet A*. 2007;143A(8):853-857. doi:10.1002/ajmg.a.31446
217. Slavotinek AM, Baranzini SE, Schanze D, et al. Manitoba-oculo-tricho-anal (MOTA) syndrome is caused by mutations in FREM1. *J Med Genet*. 2011;48(6):375-382. doi:10.1136/jmg.2011.089631
218. Neuray C, Maroofian R, Scala M, et al. Early-infantile onset epilepsy and developmental delay caused by bi-allelic GAD1 variants. *Brain*. 2020;143(8):2388-2397. doi:10.1093/brain/awaa178
219. Chatron N, Becker F, Morsy H, et al. Bi-allelic GAD1 variants cause a neonatal onset syndromic developmental and epileptic encephalopathy. *Brain*. 2020;143(5):1447-1461. doi:10.1093/brain/awaa085
220. Zhang R, Knapp M, Suzuki K, et al. ISL1 is a major susceptibility gene for classic bladder exstrophy and a regulator of urinary tract development. *Sci Rep*. 2017;7:42170. doi:10.1038/srep42170
221. Sharma A, Dakal TC, Ludwig M, Fröhlich H, Mathur R, Reutter H. Towards a central role of ISL1 in the Bladder Exstrophy-Epispadias Complex (BEEC). Computational characterisation of genetic variants and structural modelling. *Genes*. 2018;9(12). doi:10.3390/genes9120609
222. Kantarci S, Al-Gazali L, Hill RS, et al. Mutations in LRP2, which encodes the multiligand receptor megalin, cause Donnai-Barrow and facio-oculo-acoustico-renal syndromes. *Nat Genet*. 2007;39(8):957-959. doi:10.1038/ng2063
223. Khalifa O, Al-Sahlawi Z, Imtiaz F, et al. Variable expression pattern in Donnai-Barrow syndrome: report of two novel LRP2 mutations and review of the literature. *Eur J Med Genet*. 2015;58(5):293-299. doi:10.1016/j.ejmg.2014.12.008
224. Wang X, Reid Sutton V, Omar Peraza-Llanes J, et al. Mutations in X-linked PORCN, a putative regulator of Wnt signaling, cause focal dermal hypoplasia. *Nat Genet*. 2007;39(7):836-838. doi:10.1038/ng2057
225. Smigiel R, Jakubiak A, Lombardi MP, et al. Co-occurrence of severe Goltz-Gorlin syndrome and pentalogy of Cantrell—case report and review of the literature. *Am J Med Genet A*. 2011;155A:1102-1105. doi:10.1002/ajmg.a.33895

226. Maas SM, Lombardi MP, van Essen AJ, et al. Phenotype and genotype in 17 patients with Goltz-Gorlin syndrome. *J Med Genet*. 2009;46:716-720. doi:10.1136/jmg.2009.068403
227. Lombardi MP, Bulk S, Celli J, et al. Mutation update for the PORCN gene. *Hum Mutat*. 2011;32(7):723-728. doi:10.1002/humu.21505
228. Semina EV, Reiter R, Leysens NJ, et al. Cloning and characterization of a novel bicoid-related homeobox transcription factor gene, RIEG, involved in Rieger syndrome. *Nat Genet*. 1996;14:392-399. doi:10.1038/ng1296-392
229. Katz LA, Schultz RE, Semina EV, Torfs CP, Krahn KN, Murray JC. Mutations in PITX2 may contribute to cases of omphalocele and VATER-like syndromes. *Am J Med Genet A*. 2004;130A(3):277-283. doi:10.1002/ajmg.a.30329
230. Teebi AS. New autosomal dominant syndrome resembling craniofrontonasal dysplasia. *Am J Med Genet*. 1987;28(3):581-591. doi:10.1002/ajmg.1320280306
231. Kruszka P, Li D, Harr MH, et al. Mutations in SPECC1L, encoding sperm antigen with calponin homology and coiled-coil domains 1-like, are found in some cases of autosomal dominant Opitz G/BBB syndrome. *J Med Genet*. 2015;52(2):104-110. doi:10.1136/jmedgenet-2014-102677
232. Bhoj EJ, Li D, Harr MH, et al. Expanding the SPECC1L mutation phenotypic spectrum to include Teebi hypertelorism syndrome. *Am J Med Genet A*. 2015;167A(11):2497-2502. doi:10.1002/ajmg.a.37217
233. Bhoj EJ, Haye D, Toutain A, et al. Phenotypic spectrum associated with SPECC1L pathogenic variants: new families and critical review of the nosology of Teebi, Opitz GBBB, and Baraitser-Winter syndromes. *Eur J Med Genet*. 2019;62(12):103588. doi:10.1016/j.ejmg.2018.11.022
234. Rittler M, Paz JE, Castilla EE. VACTERL association, epidemiologic definition and delineation. *Am J Med Genet*. 1996;63(4):529-536.
235. Strenge S, Kujat A, Zelante L, Froster UG. A microdeletion 22q11.2 can resemble Shprintzen-Goldberg omphalocele syndrome. *Am J Med Genet A*. 2006;140(24):2838-2839. doi:10.1002/ajmg.a.31534
236. Carmi R, Barbash A, Mares AJ. The thoracoabdominal syndrome (TAS): a new X-linked dominant disorder. *Am J Med Genet*. 1990;36:109-114. doi:10.1002/ajmg.1320360122
237. Franceschini P, Guala A, Licata D, et al. Gershoni-Baruch syndrome: report of a new family confirming autosomal recessive inheritance. *Am J Med Genet A*. 2003;122A(2):174-179. doi:10.1002/ajmg.a.20275
238. Kim J, Kim P, Hui CC. The VACTERL association: lessons from the Sonic hedgehog pathway. *Clin Genet*. 2001;59(5):306-315. doi:10.1034/j.1399-0004.2001.590503.x
239. Czeizel A. New lethal omphalocele-cleft palate syndrome? *Hum Genet*. 1983;64(1):99. doi:10.1007/BF00289490
240. Stevenson RE. Common pathogenesis for sirenomelia, OEIS complex, limb-body wall defect, and other malformations of caudal structures. *Am J Med Genet A*. 2021;185(5):1379-1387. doi:10.1002/ajmg.a.62103
241. Shprintzen RJ, Goldberg RB. Dysmorphic facies, omphalocele, laryngeal and pharyngeal hypoplasia, spinal anomalies, and learning disabilities in a new dominant malformation syndrome. *Birth Defects Orig Artic Ser*. 1979;15(5B):347-353.
242. Zelante L, Germano M, Sacco M, Calvano S. Shprintzen-Goldberg omphalocele syndrome: a new patient with an expanded phenotype. *Am J Med Genet A*. 2006;140(4):383-384. doi:10.1002/ajmg.a.31064
243. Mark PR. NAD+ deficiency in human congenital malformations and miscarriage: a new model of pleiotropy. *Am J Med Genet A*. 2022;188(9):2834-2849. doi:10.1002/ajmg.a.62764
244. Cuny H, Rapadas M, Gereis J, et al. NAD deficiency due to environmental factors or gene-environment interactions causes congenital malformations and miscarriage in mice. *Proc Natl Acad Sci U S A*. 2020;117(7):3738-3747. doi:10.1073/pnas.1916588117
245. Barden CR, Lewis WH. The development of the limbs, body-wall and back in man. *Am J Anat*. 1901;1:1-36.
246. Mekonen HK, Hikspoors JP, Mommen G, Kohler SE, Lamers WH. Development of the ventral body wall in the human embryo. *J Anat*. 2015;227:673-685. doi:10.1111/joa.12380
247. Herrera AM, Cohn MJ. Embryonic origin and compartmental organization of the external genitalia. *Sci Rep*. 2014;4:6896. doi:10.1038/srep06896
248. Perriton CL, Powles N, Chiang C, Maconochie MK, Cohn MJ. Sonic hedgehog signaling from the urethral epithelium controls external genital development. *Dev Biol*. 2002;247:26-46. doi:10.1006/dbio.2002.0668
249. Haraguchi R, Mo R, Hui CC, et al. Unique functions of sonic hedgehog signaling during external genitalia development. *Development*. 2001;128:4241-4250. doi:10.1242/dev.128.21.4241
250. Haraguchi R, Suzuki K, Murakami R, et al. Molecular analysis of external genitalia formation: the role of fibroblast growth factor (Fgf) genes during genital tubercle formation. *Development*. 2000;127:2471-2479. doi:10.1242/dev.127.11.2471
251. Miyagawa S, Moon A, Haraguchi R, et al. Dosage-dependent hedgehog signals integrated with Wnt/beta-catenin signaling regulate external genitalia formation as an appendicular program. *Development*. 2009;136:3969-3978. doi:10.1242/dev.039438
252. Tschopp P, Sherratt E, Sanger TJ, et al. A relative shift in cloacal location repositions external genitalia in amniote evolution. *Nature*. 2014;516:391-394. doi:10.1038/nature13819
253. Lu MF, Pressman C, Dyer R, Johnson RL, Martin JF. Function of Rieger syndrome gene in left-right asymmetry and craniofacial development. *Nature*. 1999;401:276-278. doi:10.1038/45797
254. Delgado I, Carrasco M, Cano E, et al. GATA4 loss in the septum transversum mesenchyme promotes liver fibrosis in mice. *Hepatology*. 2014;59:2358-2370. doi:10.1002/hep.27005
255. Kuo CT, Morrisey EE, Anandappa R, et al. GATA4 transcription factor is required for ventral morphogenesis and heart tube formation. *Genes Dev*. 1997;11:1048-1060. doi:10.1101/gad.11.8.1048
256. Molkentin JD, Lin Q, Duncan SA, Olson EN. Requirement of the transcription factor GATA4 for heart tube formation and ventral morphogenesis. *Genes Dev*. 1997;11:1061-1072. doi:10.1101/gad.11.8.1061
257. Rojas A, de Val S, Heidt AB, Xu SM, Bristow J, Black BL. Gata4 expression in lateral mesoderm is downstream of BMP4 and is activated directly by Forkhead and GATA transcription factors through a distal enhancer element. *Development*. 2005;132:3405-3417. doi:10.1242/dev.01913

258. Nemer G, Nemer M. Transcriptional activation of BMP-4 and regulation of mammalian organogenesis by GATA-4 and -6. *Dev Biol*. 2003;254:131-148. doi:10.1016/s0012-1606(02)00026-x
259. Schultheiss TM, Burch JB, Lassar AB. A role for bone morphogenetic proteins in the induction of cardiac myogenesis. *Genes Dev*. 1997;11:451-462. doi:10.1101/gad.11.4.451
260. Ariza L, Carmona R, Canete A, Cano E, Munoz-Chapuli R. Coelomic epithelium-derived cells in visceral morphogenesis. *Dev Dyn*. 2016;245:307-322. doi:10.1002/dvdy.24373
261. Narita N, Bielinska M, Wilson DB. Wild-type endoderm abrogates the ventral developmental defects associated with GATA-4 deficiency in the mouse. *Dev Biol*. 1997;189:270-274. doi:10.1006/dbio.1997.8684
262. Cui Y, Jean F, Thomas G, Christian JL. BMP-4 is proteolytically activated by furin and/or PC6 during vertebrate embryonic development. *EMBO J*. 1998;17:4735-4743. doi:10.1093/emboj/17.16.4735
263. Barnes RM, Firulli BA, Conway SJ, Vincentz JW, Firulli AB. Analysis of the Hand1 cell lineage reveals novel contributions to cardiovascular, neural crest, extra-embryonic, and lateral mesoderm derivatives. *Dev Dyn*. 2010;239:3086-3097. doi:10.1002/dvdy.22428
264. Firulli AB, McFadden DG, Lin Q, Srivastava D, Olson EN. Heart and extra-embryonic mesodermal defects in mouse embryos lacking the bHLH transcription factor Hand1. *Nat Genet*. 1998;18:266-270. doi:10.1038/ng0398-266
265. Firulli BA, George RM, Harkin J, et al. HAND1 loss-of-function within the embryonic myocardium reveals survivable congenital cardiac defects and adult heart failure. *Cardiovasc Res*. 2020;116:605-618. doi:10.1093/cvr/cvz182
266. Srivastava D, Thomas T, Lin Q, Kirby ML, Brown D, Olson EN. Regulation of cardiac mesodermal and neural crest development by the bHLH transcription factor, dHAND. *Nat Genet*. 1997;16:154-160. doi:10.1038/ng0697-154
267. Kioussi C, Briata P, Baek SH, et al. Identification of a Wnt/Dvl/beta-catenin —> Pitx2 pathway mediating cell-type-specific proliferation during development. *Cell*. 2002;111:673-685. doi:10.1016/s0092-8674(02)01084-x
268. Beverdam A, Brouwer A, Reijnen M, Korving J, Meijlink F. Severe nasal clefting and abnormal embryonic apoptosis in Alx3/Alx4 double mutant mice. *Development*. 2001;128:3975-3986. doi:10.1242/dev.128.20.3975
269. Chen JM. Studies on the morphogenesis of the mouse sternum. II. Experiments on the origin of the sternum and its capacity for self-differentiation in vitro. *J Anat*. 1952;86:387-401.
270. Chen JM. Studies on the morphogenesis of the mouse sternum. I Normal embryonic development. *J Anat*. 1952;86:373-386.
271. Pourquie O, Coltey M, Breant C, Le Douarin NM. Control of somite patterning by signals from the lateral plate. *Proc Natl Acad Sci U S A*. 1995;92:3219-3223. doi:10.1073/pnas.92.8.3219
272. Pourquie O, Fan CM, Coltey M, et al. Lateral and axial signals involved in avian somite patterning: a role for BMP4. *Cell*. 1996;84:461-471. doi:10.1016/s0092-8674(00)81291-x
273. Gladstone RJ, Wakeley CP. The morphology of the sternum and its relation to the ribs. *J Anat*. 1932;66:508-564.
274. Butler MT, Wallingford JB. Planar cell polarity in development and disease. *Nat Rev Mol Cell Biol*. 2017;18:375-388. doi:10.1038/nrm.2017.11
275. Nusse R, Clevers H. Wnt/beta-catenin signaling, disease, and emerging therapeutic modalities. *Cell*. 2017;169:985-999. doi:10.1016/j.cell.2017.05.016
276. Rikitake Y, Oyama N, Wang CYC, et al. Decreased perivascular fibrosis but not cardiac hypertrophy in ROCK1+/- haploinsufficient mice. *Circulation*. 2005;112:2959-2965. doi:10.1161/CIRCULATIONAHA.105.584623
277. Duess JW, Puri P, Thompson J. Impaired cytoskeletal arrangements and failure of ventral body wall closure in chick embryos treated with rock inhibitor (Y-27632). *Pediatr Surg Int*. 2016;32:45-58. doi:10.1007/s00383-015-3811-z
278. Gabriel A, Donnelly J, Kuc A, et al. Ectopia cordis: a rare congenital anomaly. *Clin Anat*. 2014;27:1193-1199. doi:10.1002/ca.22402
279. Cantrell JR, Haller JA, Ravitch MM. A syndrome of congenital defects involving the abdominal wall, sternum, diaphragm, pericardium, and heart. *Surg Gynecol Obstet*. 1958;107:602-614.
280. Kaul B, Sheikh F, Zamora IJ, et al. 5, 4, 3, 2, 1: embryologic variants of pentalogy of Cantrell. *J Surg Res*. 2015;199:141-148. doi:10.1016/j.jss.2015.04.017
281. Carmi R, Boughman JA. Pentalogy of Cantrell and associated midline anomalies: a possible ventral midline developmental field. *Am J Med Genet*. 1992;42:90-95. doi:10.1002/ajmg.1320420118
282. Galli LM, Barnes TL, Secrest SS, Kadowaki T, Burrus LW. Porcupine-mediated lipid-modification regulates the activity and distribution of Wnt proteins in the chick neural tube. *Development*. 2007;134:3339-3348. doi:10.1242/dev.02881
283. Takada R, Satomi Y, Kurata T, et al. Monounsaturated fatty acid modification of Wnt protein: its role in Wnt secretion. *Dev Cell*. 2006;11:791-801. doi:10.1016/j.devcel.2006.10.003
284. Russo R, D'Armiento M, Angrisani P, Vecchione R. Limb body wall complex: a critical review and a nosological proposal. *Am J Med Genet*. 1993;47:893-900. doi:10.1002/ajmg.1320470617
285. Van Allen MI, Curry C, Gallagher L. Limb body wall complex: I. Pathogenesis. *Am J Med Genet*. 1987;28:529-548. doi:10.1002/ajmg.1320280302
286. Viscarello RR, Ferguson DD, Nores J, Hobbins JC. Limb-body wall complex associated with cocaine abuse: further evidence of cocaine's teratogenicity. *Obstet Gynecol*. 1992;80:523-526.
287. Bargy F, Beaudoin S. Comprehensive developmental mechanisms in gastroschisis. *Fetal Diagn Ther*. 2014;36:223-230. doi:10.1159/000360080
288. Davenport M, Haugen S, Greenough A, Nicolaides K. Closed gastroschisis: antenatal and postnatal features. *J Pediatr Surg*. 2001;36:1834-1837. doi:10.1053/jpsu.2001.28856
289. Brioude F, Kalish JM, Mussa A, et al. Expert consensus document: clinical and molecular diagnosis, screening and management of Beckwith-Wiedemann syndrome: an international consensus statement. *Nat Rev Endocrinol*. 2018;14:229-249. doi:10.1038/nrendo.2017.166
290. Phillips TM. Spectrum of cloacal exstrophy. *Semin Pediatr Surg*. 2011;20:113-118. doi:10.1053/j.sempedsurg.2010.12.007

291. Carey JC, Greenbaum B, Hall BD. The OEIS complex (omphalocele, exstrophy, imperforate anus, spinal defects). *Birth Defects Orig Artic Ser*. 1978;14:253-263.
292. Anderson JE, Cheng Y, Stephenson JT, Saadai P, Stark RA, Hirose S. Incidence of gastroschisis in California. *JAMA Surg*. 2018;153:1053-1055. doi:10.1001/jamasurg.2018.1744
293. Vu LT, Nobuhara KK, Laurent C, Shaw GM. Increasing prevalence of gastroschisis: population-based study in California. *J Pediatr*. 2008;152:807-811. doi:10.1016/j.jpeds.2007.11.037
294. Liu S, Evans J, Boutin A, et al. Time trends, geographic variation and risk factors for gastroschisis in Canada: a population-based cohort study 2006-2017. *Paediatr Perinat Epidemiol*. 2021;35:664-673. doi:10.1111/ppe.12800
295. Kelay A, Durkin N, Davenport M. Congenital anterior abdominal wall defects. *Surgery (Oxford)*. 2016;34:621-627.
296. Springett A, Draper ES, Rankin J, et al. Birth prevalence and survival of exomphalos in England and Wales: 2005 to 2011. *Birth Defects Res A Clin Mol Teratol*. 2014;100:721-725. doi:10.1002/bdra.23301
297. Mac Bird T, Robbins JM, Druschel C, Cleves MA, Yang S, Hobbs CA. Demographic and environmental risk factors for gastroschisis and omphalocele in the National Birth Defects Prevention Study. *J Pediatr Surg*. 2009;44:1546-1551. doi:10.1016/j.jpedsurg.2008.10.109
298. Lakasing L, Cicero S, Davenport M, Patel S, Nicolaides KH. Current outcome of antenatally diagnosed exomphalos: an 11 year review. *J Pediatr Surg*. 2006;41:1403-1406. doi:10.1016/j.jpedsurg.2006.04.015
299. Draper ES, Rankin J, Tonks AM, et al. Recreational drug use: a major risk factor for gastroschisis? *Am J Epidemiol*. 2008;167:485-491. doi:10.1093/aje/kwm335
300. David AL, Holloway A, Thomasson L, et al. A case-control study of maternal periconceptual and pregnancy recreational drug use and fetal malformation using hair analysis. *PLoS One*. 2014;9:e111038. doi:10.1371/journal.pone.0111038
301. Torfs CP, Katz EA, Bateson TF, Lam PK, Curry CJ. Maternal medications and environmental exposures as risk factors for gastroschisis. *Teratology*. 1996;54:84-92. doi:10.1002/(SICI)1096-9926(199606)54:23.0.CO;2-4
302. Spinder N, Almli LM, Desrosiers TA, et al. Maternal occupational exposure to solvents and gastroschisis in offspring—National Birth Defects Prevention Study 1997-2011. *Occup Environ Med*. 2020;77:172-178. doi:10.1136/oemed-2019-106147
303. Paranjothy S, Broughton H, Evans A, et al. The role of maternal nutrition in the aetiology of gastroschisis: an incident case-control study. *Int J Epidemiol*. 2012;41:1141-1152. doi:10.1093/ije/dys092
304. Mattix KD, Winchester PD, Scherer LR. Incidence of abdominal wall defects is related to surface water atrazine and nitrate levels. *J Pediatr Surg*. 2007;42:947-949. doi:10.1016/j.jpedsurg.2007.01.027
305. Dolk H, Armstrong B, Lachowycz K, et al. Ambient air pollution and risk of congenital anomalies in England, 1991-1999. *Occup Environ Med*. 2010;67:223-227. doi:10.1136/oem.2009.045997
306. Li LL, Huang YH, Li J, et al. Maternal exposure to sulfur dioxide and risk of Omphalocele in Liaoning Province, China: a population-based case-control study. *Front Public Health*. 2022;10:821905. doi:10.3389/fpubh.2022.821905
307. Chang S, Bartolomei MS. Modeling human epigenetic disorders in mice: Beckwith-Wiedemann syndrome and Silver-Russell syndrome. *Dis Model Mech*. 2020;13. doi:10.1242/dmm.044123
308. Rentsendorj A, Mohan S, Szabo P, Mann JR. A genomic imprinting defect in mice traced to a single gene. *Genetics*. 2010;186:917-927. doi:10.1534/genetics.110.118802
309. Martin RA, Cunniff C, Erickson L, Jones KL. Pentalogy of Cantrell and ectopia cordis, a familial developmental field complex. *Am J Med Genet*. 1992;42:839-841. doi:10.1002/ajmg.1320420619
310. Langlois D, Hneino M, Bouazza L, et al. Conditional inactivation of TGF-beta type II receptor in smooth muscle cells and epicardium causes lethal aortic and cardiac defects. *Transgenic Res*. 2010;19:1069-1082. doi:10.1007/s11248-010-9379-4
311. Grzeschik KH, Bornholdt D, Oeffner F, et al. Deficiency of PORCN, a regulator of Wnt signaling, is associated with focal dermal hypoplasia. *Nat Genet*. 2007;39:833-835. doi:10.1038/ng2052
312. Song H, Hu J, Chen W, et al. Planar cell polarity breaks bilateral symmetry by controlling ciliary positioning. *Nature*. 2010;466:378-382. doi:10.1038/nature09129
313. Chikkannaiah P, Dhumale H, Kangle R, Shekar R. Limb body wall complex: a rare anomaly. *J Lab Phys*. 2013;5:65-67. doi:10.4103/0974-2727.115930
314. Ge G, Greenspan DS. Developmental roles of the BMP1/TLD metalloproteinases. *Birth Defects Res C Embryo Today*. 2006;78:47-68. doi:10.1002/bdrc.20060
315. Tumelty KE, Smith BD, Nugent MA, Layne MD. Aortic carboxypeptidase-like protein (ACLP) enhances lung myofibroblast differentiation through transforming growth factor beta receptor-dependent and -independent pathways. *J Biol Chem*. 2014;289:2526-2536. doi:10.1074/jbc.M113.502617
316. Vadon-Le Goff S, Hulmes DJ, Moali C. BMP-1/tolloid-like proteinases synchronize matrix assembly with growth factor activation to promote morphogenesis and tissue remodeling. *Matrix Biol*. 2015;44-46:14-23. doi:10.1016/j.matbio.2015.02.006
317. Van Dorp DR, Malleis JM, Sullivan BP, Klein MD. Teratogens inducing congenital abdominal wall defects in animal models. *Pediatr Surg Int*. 2010;26:127-139. doi:10.1007/s00383-009-2482-z
318. Blackburn PR, Xu Z, Tumelty KE, et al. Bi-allelic alterations in AEBP1 lead to defective collagen assembly and connective tissue structure resulting in a variant of Ehlers-Danlos syndrome. *Am J Hum Genet*. 2018;102:696-705. doi:10.1016/j.ajhg.2018.02.018
319. Ritelli M, Colombi M. Molecular genetics and pathogenesis of Ehlers-Danlos syndrome and related connective tissue disorders. *Genes*. 2020;11:547. doi:10.3390/genes11050547
320. Perveen R, Lloyd IC, Clayton-Smith J, et al. Phenotypic variability and asymmetry of Rieger syndrome associated with PITX2 mutations. *Invest Ophthalmol Vis Sci*. 2000;41:2456-2460.
321. Hjalt TA, Amendt BA, Murray JC. PITX2 regulates procollagen lysyl hydroxylase (PLOD) gene expression: implications for the pathology of Rieger syndrome. *J Cell Biol*. 2001;152:545-552. doi:10.1083/jcb.152.3.545
322. Ludwig M, Ching B, Reutter H, Boyadjiev SA. Bladder exstrophy-epispadias complex. *Birth Defects Res A Clin Mol Teratol*. 2009;85:509-522. doi:10.1002/bdra.20557

323. Beaman GM, Cervellione RM, Keene D, Reutter H, Newman WG. The genomic architecture of bladder exstrophy epispadias complex. *Genes*. 2021;12:1149. doi:10.3390/genes12081149
324. Reutter H, Keppler-Noreuil K, Keegan CE, Thiele H, Yamada G, Ludwig M. Genetics of bladder-exstrophy-epispadias complex (BEEC): systematic elucidation of Mendelian and multifactorial phenotypes. *Curr Genomics*. 2016;17:4-13. doi:10.2174/1389202916666151014221806
325. Ching BJ, Wittler L, Proske J, et al. p63 (TP73L) a key player in embryonic urogenital development with significant dysregulation in human bladder exstrophy tissue. *Int J Mol Med*. 2010;26:861-867. doi:10.3892/ijmm_00000535
326. Wilkins S, Zhang KW, Mahfuz I, et al. Insertion/deletion polymorphisms in the DeltaNp63 promoter are a risk factor for bladder exstrophy epispadias complex. *PLoS Genet*. 2012;8:e1003070. doi:10.1371/journal.pgen.1003070
327. Li Y, Giovannini S, Wang T, et al. p63: a crucial player in epithelial stemness regulation. *Oncogene*. 2023;42:3371-3384. doi:10.1038/s41388-023-02859-4
328. Osler W, Paton S, Thayer WS. Jesse William Lazear memorial. *Science*. 1901;14:225. doi:10.1126/science.14.345.225
329. Straub E, Spranger J. Etiology and pathogenesis of the prune belly syndrome. *Kidney Int*. 1981;20:695-699. doi:10.1038/ki.1981.198
330. Prummel KD, Nieuwenhuize S, Mosimann C. The lateral plate mesoderm. *Development*. 2020;147. doi:10.1242/dev.175059
331. Granberg CF, Harrison SM, Dajusta D, et al. Genetic basis of prune belly syndrome: screening for HNF1beta gene. *J Urol*. 2012;187:272-278. doi:10.1016/j.juro.2011.09.036
332. Boghossian NS, Sicko RJ, Giannakou A, et al. Rare copy number variants identified in prune belly syndrome. *Eur J Med Genet*. 2018;61:145-151. doi:10.1016/j.ejmg.2017.11.008
333. Coffinier C, Barra J, Babinet C, Yaniv M. Expression of the vHNF1/HNF1beta homeoprotein gene during mouse organogenesis. *Mech Dev*. 1999;89:211-213. doi:10.1016/s0925-4773(99)00221-x
334. Nishinakamura R, Sakaguchi M. BMP signaling and its modifiers in kidney development. *Pediatr Nephrol*. 2014;29:681-686. doi:10.1007/s00467-013-2671-9
335. Galea GL, Maniou E, Edwards TJ, et al. Cell non-autonomy amplifies disruption of neurulation by mosaic Vangl2 deletion in mice. *Nat Commun*. 2021;12:1159. doi:10.1038/s41467-021-21372-4

SUPPORTING INFORMATION

Additional supporting information can be found online in the Supporting Information section at the end of this article.

How to cite this article: Formstone C, Aldeiri B, Davenport M, Francis-West P. Ventral body wall closure: Mechanistic insights from mouse models and translation to human pathology. *Developmental Dynamics*. 2024;1-40. doi:10.1002/dvdy.735